

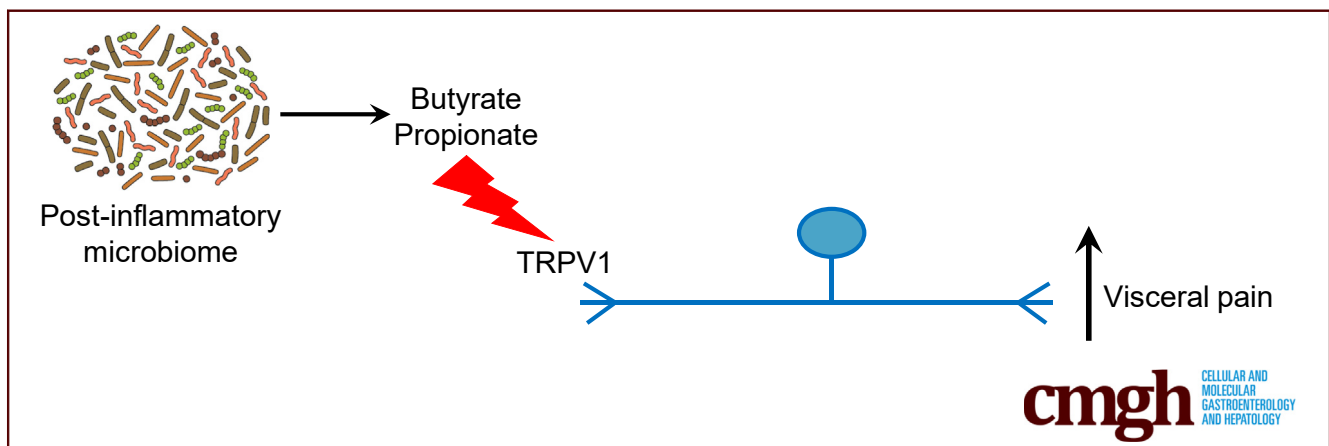
## ORIGINAL RESEARCH

## Colitis-Induced Microbial Perturbation Promotes Postinflammatory Visceral Hypersensitivity



Nicolas Esquerre,<sup>1</sup> Lilian Basso,<sup>1,2</sup> Manon Defaye,<sup>1,2</sup> Fernando A. Vicentini,<sup>1,2,3</sup> Nina Cluny,<sup>1,2,3</sup> Dominique Bihan,<sup>4</sup> Simon A. Hirota,<sup>1,2</sup> Alana Schick,<sup>5</sup> Humberto B. Jijon,<sup>1,6</sup> Ian A. Lewis,<sup>4</sup> Markus B. Geuking,<sup>1,7</sup> Keith A. Sharkey,<sup>1,2,3</sup> Christophe Altier,<sup>1,2,8</sup> and Yasmin Nasser<sup>1,6</sup>

<sup>1</sup>Snyder Institute for Chronic Diseases, Cumming School of Medicine, University of Calgary; <sup>3</sup>Hotchkiss Brain Institute, Cumming School of Medicine, University of Calgary; <sup>2</sup>Department of Physiology and Pharmacology, Cumming School of Medicine, University of Calgary; <sup>4</sup>Department of Biological Sciences, University of Calgary; <sup>5</sup>International Microbiome Centre, Cumming School of Medicine, University of Calgary; <sup>6</sup>Division of Gastroenterology and Hepatology, Department of Medicine, University of Calgary; <sup>7</sup>Department of Microbiology, Immunity and Infectious Diseases, Cumming School of Medicine, University of Calgary; and <sup>8</sup>Alberta Children's Hospital Research Institute, Cumming School of Medicine, University of Calgary, Calgary, Alberta, Canada



## SUMMARY

Our understanding of the pathophysiological mechanisms underlying chronic pain in inflammatory bowel disease is incomplete. Here we show that microbial manipulation modulates the development of visceral, but not somatic, pain in a mouse model of postinflammatory dextran sodium sulfate colitis.

**BACKGROUND & AIMS:** Despite achieving endoscopic remission, more than 20% of inflammatory bowel disease patients experience chronic abdominal pain. These patients have increased rectal transient receptor potential vanilloid-1 receptor (TRPV1) expression, a key transducer of inflammatory pain. Because inflammatory bowel disease patients in remission exhibit dysbiosis and microbial manipulation alters TRPV1 function, our goal was to examine whether microbial perturbation modulated transient receptor potential function in a mouse model.

**METHODS:** Mice were given dextran sodium sulfate (DSS) to induce colitis and were allowed to recover. The microbiome was perturbed by using antibiotics as well as fecal microbial

transplant (FMT). Visceral and somatic sensitivity were assessed by recording visceromotor responses to colorectal distention and using hot plate/automated Von Frey tests, respectively. Calcium imaging of isolated dorsal root ganglia neurons was used as an in vitro correlate of nociception. The microbiome composition was evaluated via 16S rRNA gene variable region V4 amplicon sequencing, whereas fecal short-chain fatty acids (SCFAs) were assessed by using targeted mass spectrometry.

**RESULTS:** Postinflammatory DSS mice developed visceral and somatic hyperalgesia. Antibiotic administration during DSS recovery induced visceral, but not somatic, hyperalgesia independent of inflammation. FMT of postinflammatory DSS stool into antibiotic-treated mice increased visceral hypersensitivity, whereas FMT of control stool reversed antibiotics' sensitizing effects. Postinflammatory mice exhibited both increased SCFA-producing species and fecal acetate/butyrate content compared with controls. Capsaicin-evoked calcium responses were increased in naive dorsal root ganglion neurons incubated with both sodium butyrate/propionate alone and with colonic supernatants derived from postinflammatory mice.

**CONCLUSIONS:** The microbiome plays a central role in postinflammatory visceral hypersensitivity. Microbial-derived

SCFAs can sensitize nociceptive neurons and may contribute to the pathogenesis of postinflammatory visceral pain. (*Cell Mol Gastroenterol Hepatol* 2020;10:225–244; <https://doi.org/10.1016/j.jcmgh.2020.04.003>)

**Keywords:** Microbiome; Visceral Pain; DSS Colitis; Dorsal Root Ganglion; Short-Chain Fatty Acids; Calcium Imaging.

Inflammatory bowel diseases (IBDs), including Crohn's disease and ulcerative colitis, are chronic, debilitating illnesses with high socioeconomic burden and increasing prevalence.<sup>1</sup> Despite achieving endoscopic remission, more than 20% of IBD patients experience chronic abdominal pain,<sup>2,3</sup> which is associated with high levels of anxiety, depression and poor quality of life.<sup>2,4,5</sup> Furthermore, studies demonstrate increased prevalence of widespread somatic pain in the absence of inflammation in IBD,<sup>6</sup> indicating altered sensory neural processing in this condition.<sup>3</sup> Unfortunately, effective treatments for chronic pain are severely limited, such that 5%–25% of IBD patients are on chronic narcotic therapy, use of which is not only ineffectual but leads to increased mortality.<sup>3,7</sup>

The gut microbiome affects a wide variety of gastrointestinal processes.<sup>8</sup> There is evidence that some IBD patients in remission exhibit persistent changes in the microbiome,<sup>9–14</sup> although it is not known whether these changes are a cause or consequence of previous inflammation, dietary changes, or altered gastrointestinal transit.<sup>8</sup> IBD patients in endoscopic remission with chronic pain exhibit elevated rectal transient receptor potential vanilloid-1 receptor (TRPV1) expression, which correlated with the severity of abdominal pain.<sup>15</sup> Interestingly, there is evidence that microbial products can directly stimulate nociceptors<sup>16–20</sup> via TRP channels,<sup>21</sup> whereas microbial manipulation results in altered function and expression of molecular targets in pain signaling such as TRPV1.<sup>22,23</sup> This suggests a potential link between dysbiosis and chronic visceral pain in the absence of inflammation in IBD through the microbial modulation of TRP receptors.

Our goal was to examine whether microbial perturbation in the postinflammatory state contributed to persistent visceral hypersensitivity. We chose to use the postinflammatory dextran sodium sulfate (DSS) mouse model of colitis because this is an established animal model of chronic visceral pain, in which animals display increased visceral hypersensitivity 5 weeks after DSS administration in the absence of inflammation.<sup>24</sup> Postinflammatory visceral hyperalgesia was found to be dependent on TRPV1 in this model, because TRPV1 expression in afferent nerves was elevated in the postinflammatory state,<sup>24–26</sup> similar to IBD patients in endoscopic remission with chronic pain.<sup>15</sup> We also examined somatic pain in this model because of the data demonstrating increased prevalence of non-inflammatory somatic pain in IBD.<sup>6,27</sup> To manipulate the microbiome, we administered a broad-spectrum antibiotic cocktail to mice<sup>28</sup> and also performed fecal microbial transplant (FMT).<sup>29,30</sup> We set out to test whether the dysbiotic microbiome in the postinflammatory state drives

nociceptor sensitization through TRPV1 regulation and thus may contribute to the transition from acute to chronic pain.

## Results


### *Postinflammatory Microbial Perturbation Leads to Visceral Hyperalgesia But Not Somatic Hypersensitivity*

To evaluate the effects of inflammation-induced microbial perturbation on visceral pain, mice were treated with 2.5% DSS in the drinking water for 5 days (DSS) or water alone (control [CT]) and allowed to recover for 5 weeks (Figure 1A). These mice were divided into 2 subgroups and treated with antibiotics (Abx) for the last 2 weeks of recovery (CT + Abx; DSS + Abx). Mice exposed to DSS showed signs of clinical disease including significant weight loss (Figure 1B) and loose stools but recovered after 5 weeks and did not exhibit macroscopic or microscopic intestinal inflammation at the time of death, as previously described<sup>24</sup> (Figure 1C–E). Similarly, Abx treatment did not result in any macroscopic inflammation (Figure 1C and D).

The visceromotor response to colorectal distention was increased in postinflammatory DSS mice when compared with control mice given water only, similar to that seen previously<sup>24</sup> (area under the curve for colorectal distention: control,  $0.1 \pm 0.01$  vs DSS,  $0.16 \pm 0.01$ ;  $P < .01$ ; Figure 2A). Microbial disruption with Abx during colitis recovery induced visceral allodynia and hyperalgesia in Abx-treated mice (visceromotor response at 30 mm Hg: control,  $0.01 \pm 0.03$  vs control + Abx,  $0.05 \pm 0.0$ ;  $P < .05$ ; area under the curve for colorectal distention: control,  $0.1 \pm 0.01$  vs DSS + Abx,  $0.22 \pm 0.04$ ;  $P < .01$ ; Figure 2A), independent of DSS treatment.

To determine whether microbial manipulation was able to modulate somatic pain, we assessed both mechanical and thermal hypersensitivity in animals treated with DSS and Abx. Mechanical sensitivity was assessed by using the automated Von Frey test in the hind paw, and thermal sensitivity was evaluated by using the hot plate test. Mice treated with DSS developed somatic hyperalgesia in both mechanical (Von Frey test force: control,  $7.7 \pm 0.24$  g vs DSS,  $6 \pm 0.23$  g;  $P < .0001$ ; control + Abx,  $8.1 \pm 0.25$  g vs DSS + Abx,  $6.6 \pm 0.19$  g;  $P < .001$ ; Figure 2B) and thermal (time on  $52^\circ\text{C}$  hot plate: control,  $10.6 \pm 0.51$  seconds vs DSS,  $7.9 \pm 0.40$  seconds;  $P < .001$ ; control + Abx,  $10.8 \pm 0.37$  seconds

**Abbreviations used in this paper:** Abx, antibiotics; ASV, amplicon sequence variant; DMEM, Dulbecco modified Eagle medium; DRG, dorsal root ganglion; DSS, dextran sulfate sodium; FMT, fecal microbial transplant; HBSS, Hanks' balanced salt solution; IBD, inflammatory bowel disease; IBS, irritable bowel syndrome; PBS, phosphate-buffered saline; PCR, polymerase chain reaction; SCFA, short-chain fatty acid; TRPA1, transient receptor potential ankyrin-1 receptor; TRPV1, transient receptor potential vanilloid-1 receptor.

 Most current article

© 2020 The Authors. Published by Elsevier Inc. on behalf of the AGA Institute. This is an open access article under the CC BY-NC-ND license (<http://creativecommons.org/licenses/by-nc-nd/4.0/>).

2352-345X

<https://doi.org/10.1016/j.jcmgh.2020.04.003>

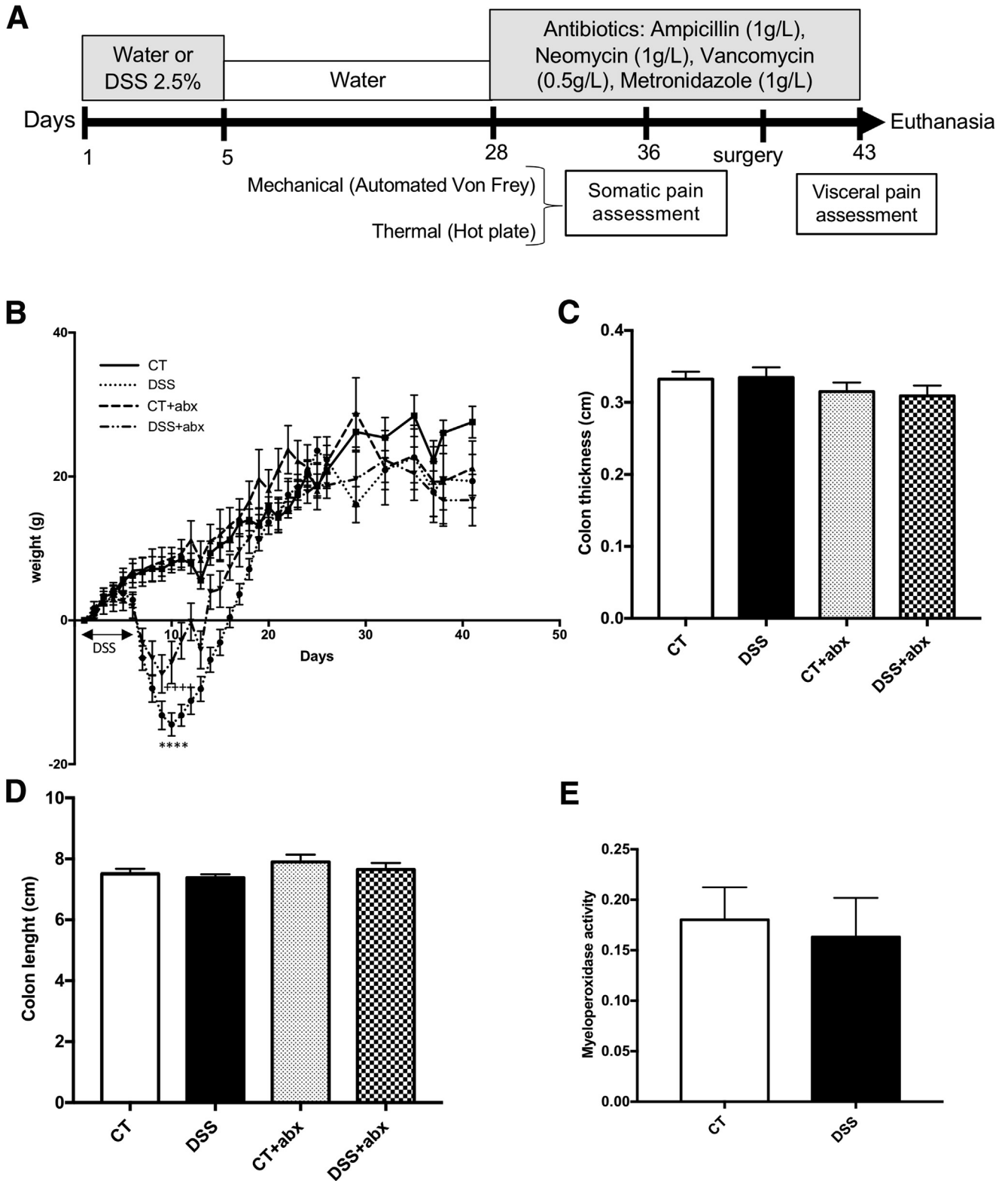


**Figure 1. Postinflammatory DSS mice exhibit no signs of macroscopic or microscopic inflammation. (A) Experimental protocol.** Colitis was induced using 2.5% DSS for 5 days. Mice were allowed to recover for 3 weeks and then antibiotics (Abx) were administered in drinking water for 2 weeks before death. (B) DSS-treated animals initially lose weight but catch up to their control counterparts. Two-way analysis of variance, control (CT) vs DSS, \*\*\*\* $P < .0001$ ; CT vs DSS + Abx, ++++ $P < .0001$ . Controls (CT):  $n = 12$ , DSS:  $n = 15$ , CT + Abx:  $n = 11$ , DSS + Abx:  $n = 10$ . Macroscopic inflammation was assessed by using colon thickness (C) and length (D). CT:  $n = 17$ , DSS:  $n = 20$ , CT + Abx and DSS + Abx,  $n = 8$ . Microscopic inflammation was assessed by myeloperoxidase activity quantification (E) between control ( $n = 10$ ) and DSS ( $n = 7$ ) groups. DSS, dextran sulfate sodium.

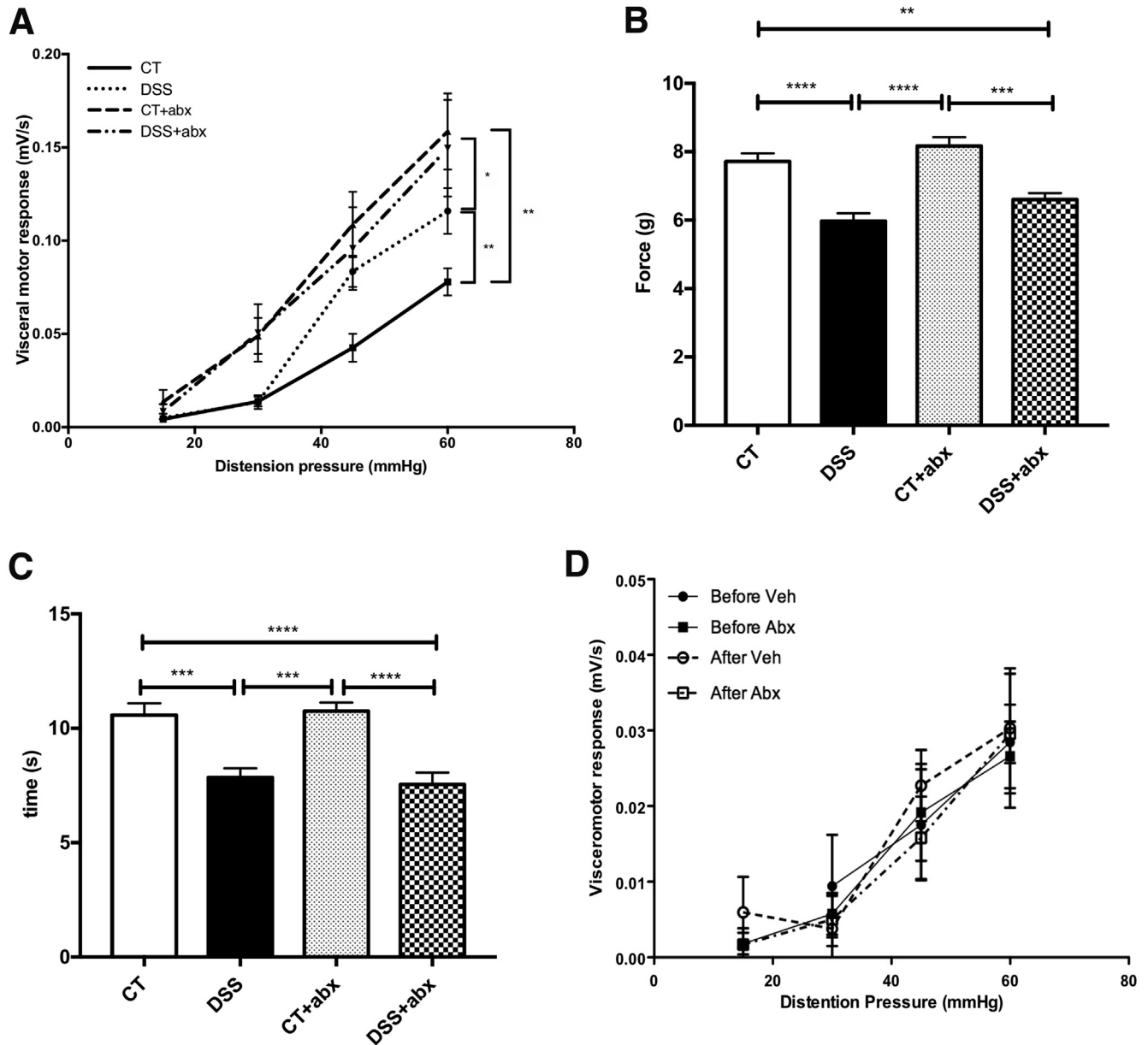


**Figure 2. Postinflammatory DSS mice exhibit both visceral and somatic hyperalgesia.** (A) Visceral pain was assessed by using the visceromotor response to colorectal distention. Kruskal-Wallis test of area under the curve:  $*P < .05$ ;  $**P < .01$ . Controls (CT):  $n = 15$ , DSS:  $n = 15$ , CT + Abx:  $n = 13$ , and DSS + Abx:  $n = 15$ , 4 experiments). Somatic pain was assessed 7 days before death by using the automated Von Frey (mechanical, B) and hot plate tests (thermal, C). One-way analysis of variance:  $**P < .01$ ;  $***P < .001$ ,  $****P < .0001$  (CT:  $n = 15$ , DSS and DSS + Abx:  $n = 10$ , CT + Abx:  $n = 13$  for the automated Von Frey test. CT and DSS:  $n = 15$ , CT + Abx:  $n = 16$ , and DSS + Abx:  $n = 10$  for the hot plate test, 4 experiments). (D) Visceromotor responses were tested before and 1 hour after administration of saline (Vehicle, Veh) or antibiotics into the colon via a double-lumen catheter. No differences were noted in visceral sensitivity before or after administration of saline or antibiotics. Abx, antibiotics; DSS, dextran sulfate sodium.

vs DSS + Abx,  $7.5 \pm 0.40$  seconds;  $P < .0001$ ; Figure 2C) tests independent of Abx treatment.

To evaluate whether Abx exerted a direct effect on visceral pain, and visceromotor responses were tested before and 1 hour after administration of either vehicle (sterile saline) or Abx into the colon.<sup>31</sup> No differences were seen in visceral sensitivity between groups (area under the curve for colorectal distention: before vehicle:  $0.63 \pm 0.20$ , after vehicle:  $0.73 \pm 0.14$ , before

Abx:  $0.59 \pm 0.13$ , after Abx:  $0.73 \pm 0.14$ ; one-way analysis of variance,  $P = .65$ ;  $n = 6$ /group; Figure 2D).

### Microbial Reconstitution After Antibiotics Treatment Reverses Changes in Visceral, But Not Somatic, Hyperalgesia

To assess the role of Abx-induced microbial disruption in visceral pain, Abx-treated animals were given a 2-week

washout period in which they were given water only (Figure 3A). Seven weeks after DSS, the visceromotor response to colorectal distention in postinflammatory DSS mice was still significantly higher than controls (area under the curve for colorectal distention: control,  $0.07 \pm 0.01$  vs DSS,  $0.15 \pm 0.04$ ;  $P < .05$ ; Figure 3B). Interestingly, visceral hypersensitivity recovered to control levels in control + Abx and DSS + Abx mice after 2 weeks of Abx washout. However, somatic hyperalgesia was unaffected by Abx washout (Figure 3C and D; Von Frey test force: control,  $7.4 \pm 0.16$  g vs DSS,  $5.5 \pm 0.11$  g;  $P < .001$ ; control + Abx,  $7.2 \pm 0.27$  g vs DSS + Abx,  $5.8 \pm 0.12$  g;  $P < .001$ ; time on 52°C hot plate: control,  $13 \pm 0.8$  seconds vs DSS,  $10.2 \pm 0.6$  seconds;  $P < .05$ ; control + Abx,  $13.9 \pm 0.71$  seconds vs DSS + Abx,  $10.2 \pm 0.34$  seconds;  $P < .01$ ), suggesting that microbial manipulation modulates the development of visceral, but not somatic, pain.

### Gut Microbiota and Stool Short-Chain Fatty Acid Content Differ Between Control and Postinflammatory Dextran Sulfate Sodium Mice

Microbes and bacterial metabolites such as short-chain fatty acid (SCFA) are known to activate intestinal epithelial cells and extrinsic spinal neurons,<sup>16–19,32,33</sup> suggesting that they may play a role in visceral hypersensitivity. Stool was collected from mice at baseline and at the time of death for microbial composition and SCFA analysis.

Examination of the microbiome composition demonstrated that the alpha and beta diversity were not significantly different when comparing control and postinflammatory DSS mice at the 5-week recovery time point, whereas Abx treatment resulted in a marked disruption characterized by a shift in both alpha and beta diversity at the operational taxonomic unit level ( $n = 6$ /group except DSS + Abx baseline,  $n = 7$ ; control baseline,  $n = 5$ ; and DSS + Abx group at death,  $n = 4$ ; alpha diversity: linear mixed-effects model,  $P = .0072$ ; beta diversity: permutational multivariate analysis of variance,  $P < .001$ ; Figure 4A and B). When compared at the phylum and genus levels, the composition of all 4 groups was similar at baseline (Figure 4C). As expected, Abx treatment resulted in profound shifts in the microbiota characterized by an overgrowth of proteobacteria, primarily *Klebsiella* species (Figure 4C; beta-binomial regression,  $P < .01$ ). Examined at the 5-week recovery period, DSS treatment resulted in a relative decrease in Bacteroidetes and an increase in Firmicutes phylum compared with controls, as previously described<sup>34</sup> (Figure 4D); in addition, an increase in *Verrucomicrobia*, which has been linked with gut health in some studies,<sup>35,36</sup> was seen over time in controls. At the genus level, a significant increase in *Lachnospiraceae* NK4A136 and FCS020 groups as well as *Ruminococcus* was seen, whereas a significant decrease in *Akkermansia*, *Alistipes*, *Muribaculaceae*, *Ruminococcaceae*, and *Bacteroides* species was apparent in postinflammatory DSS mice when compared with controls (Figure 4D; beta-binomial regression,  $P < .01$ ). After antibiotic washout (Figure 3A), there was partial recovery of the microbiome in Abx-treated mice

(Figure 5A and B) at the 7-week time point. However, DSS treatment resulted in a persistent increase in *Lachnospiraceae* NK4A136 and FCS020 groups as well as *Ruminococcus* groups at the 7-week time point (Figure 5C) when compared with controls.

The subtle microbial perturbation observed in postinflammatory DSS mice was associated with an increase in fecal acetate (acetate [mmol/L]: control,  $2.2 \pm 0.02$  vs DSS,  $4.4 \pm 0.1$ ;  $P < .05$ ) and butyrate (butyrate [mmol/L]: control,  $1 \pm 0.02$  vs DSS,  $2.3 \pm 0.04$ ;  $P < .05$ ) but not propionate when compared with controls (Figure 6A). SCFA concentration was below the limit of detection in Abx-treated animals. After antibiotic washout, SCFA concentration in Abx-treated animals was detectable but significantly lower for butyrate and propionate compared with the control and DSS groups, respectively (Figure 6B), suggesting partial restoration after Abx washout. No differences were observed between control and DSS groups.

### Fecal Microbial Transplantation of Postinflammatory Dextran Sulfate Sodium Microbiota Transfers the Phenotype of Visceral, But Not Somatic, Pain

To determine whether the dysbiotic microbiome was necessary for the expression of visceral hypersensitivity, we performed FMT experiments. Mice were treated with 2 weeks of Abx before FMT to disrupt the basal microbiome (Figure 7A). Twenty-four hours after the cessation of Abx, mice received 4 days of oral gavage with homogenized stool derived from control mice, postinflammatory DSS mice, or vehicle alone (phosphate-buffered saline [PBS] + glycerol). Animals treated with postinflammatory DSS stools developed visceral hypersensitivity compared with mice given vehicle or control stool (area under the curve for colorectal distention: FMT PBS,  $0.06 \pm 0.007$  vs FMT DSS,  $0.12 \pm 0.02$ ;  $P < .01$ ; FMT control,  $0.05 \pm 0.006$  vs FMT DSS,  $0.12 \pm 0.02$ ;  $P < .001$ ; Figure 7B). Interestingly, mice given vehicle displayed hyperalgesia at 60 mm Hg compared with mice given control stool (visceromotor response at 60 mm Hg: FMT control,  $0.03 \pm 0.004$  vs FMT PBS,  $0.06 \pm 0.007$ ;  $P < .05$ ; Figure 7B), suggesting that the sensitizing effect of Abx alone on visceral sensitivity could be reversed by FMT from control mice. In contrast, FMT did not transfer somatic hypersensitivity observed in postinflammatory mice (Figure 7C and D), suggesting that the microbiome plays a central role in the pathogenesis of postinflammatory visceral, but not somatic, hypersensitivity.

Examination of the SCFA profile of recipient mice revealed that FMT was associated with an increase in fecal propionate (propionate [mmol/L]: FMT PBS,  $0.147 \pm 0.044$  vs FMT DSS,  $0.6 \pm 0.087$ ;  $P < .0001$ ; FMT control,  $0.337 \pm 0.041$  vs FMT DSS,  $0.6 \pm 0.087$ ;  $P < .05$ ) and butyrate (butyrate [mmol/L]: FMT PBS,  $0.073 \pm 0.028$  vs FMT DSS,  $0.509 \pm 0.103$ ;  $P < .001$ ; FMT control,  $0.144 \pm 0.021$  vs FMT DSS,  $0.509 \pm 0.103$ ;  $P < .01$ ) in the stool of recipients given postinflammatory DSS stool compared with those given vehicle or control stool (Figure 7E). These data suggest that postinflammatory visceral hypersensitivity is associated

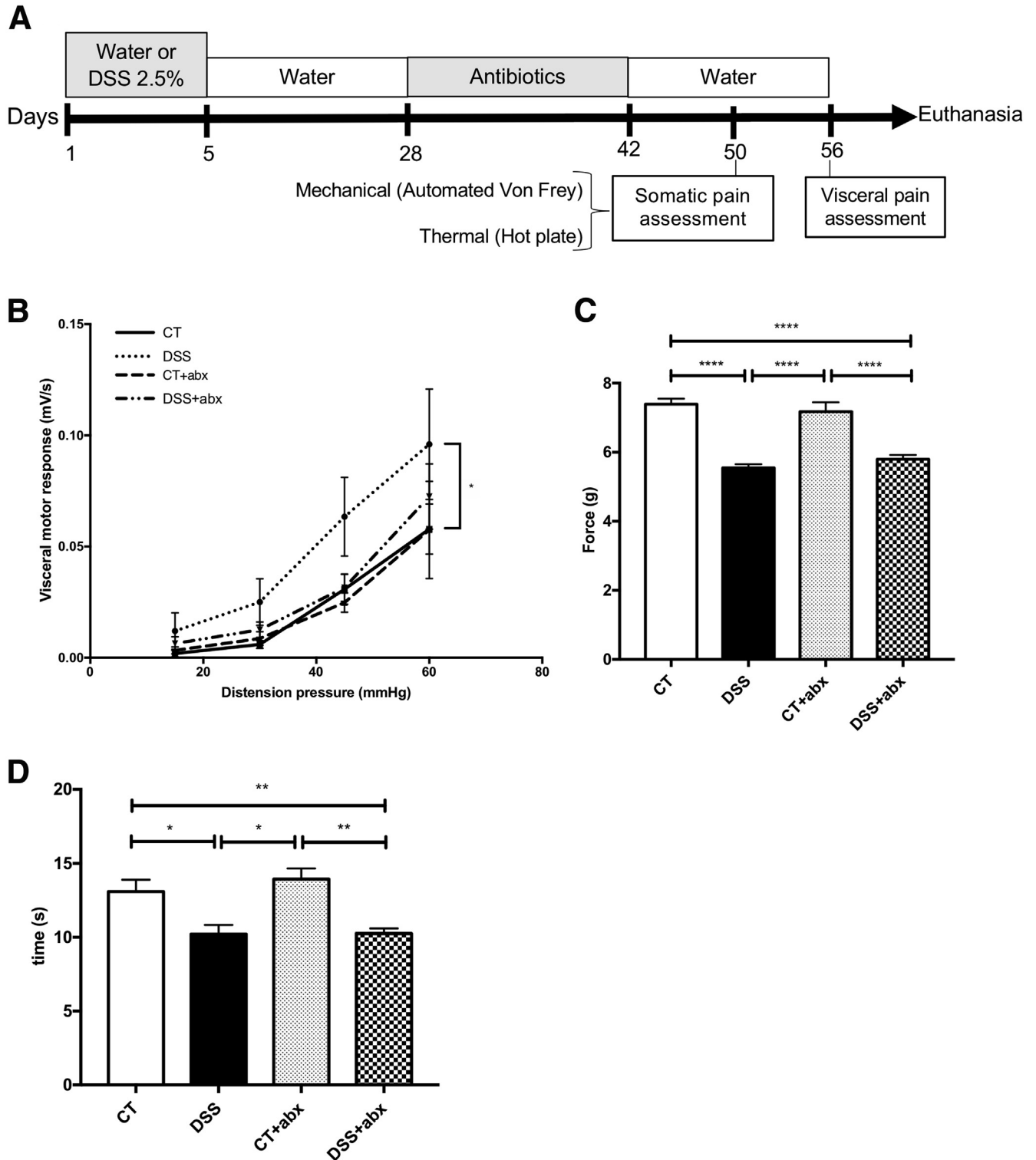
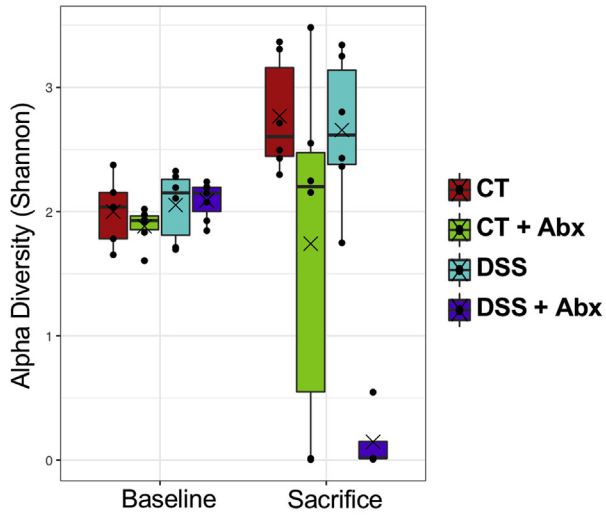
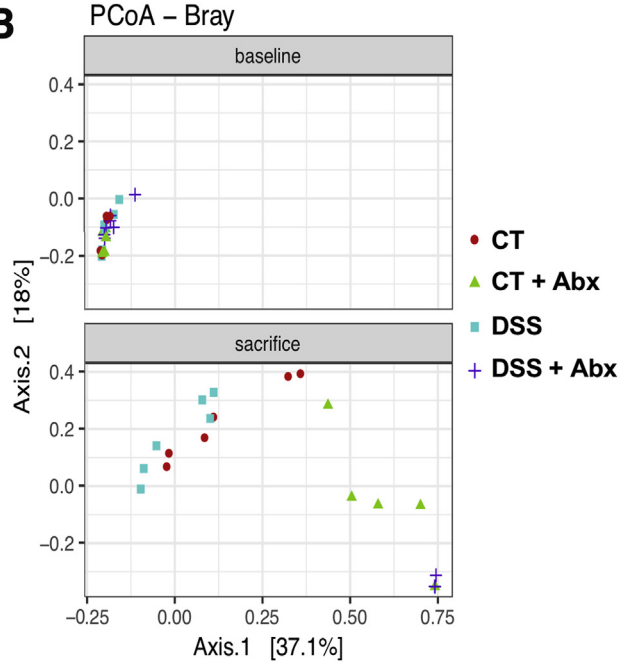


**Figure 3. Microbial recovery after antibiotic administration reverses changes in visceral hyperalgesia. (A) Experimental protocol.** Colitis was induced by using 2.5% DSS for 5 days, and animals were allowed to recover. Antibiotics (Abx) were administered in drinking water from days 28–42; animals were then given a 2-week washout period. **(B)** Visceral pain was assessed by using the visceromotor response to colorectal distention. One-way analysis of variance of area under the curve of DSS vs CT:  $*P < .05$ . CT:  $n = 11$ , CT + Abx and DSS:  $n = 12$ , DSS + Abx:  $n = 15$ . Somatic pain was assessed by using the automated Von Frey **(C)** and hot plate **(D)** tests. One-way analysis of variance:  $*P < .05$ ;  $**P < .01$ ;  $***P < .001$ ;  $****P < .0001$ . CT and DSS:  $n = 7$ ; CT + Abx and DSS + Abx:  $n = 8$  for automated Von Frey test and  $n = 14$ /group for hot plate test (4 experiments). CT, control; DSS, dextran sulfate sodium.

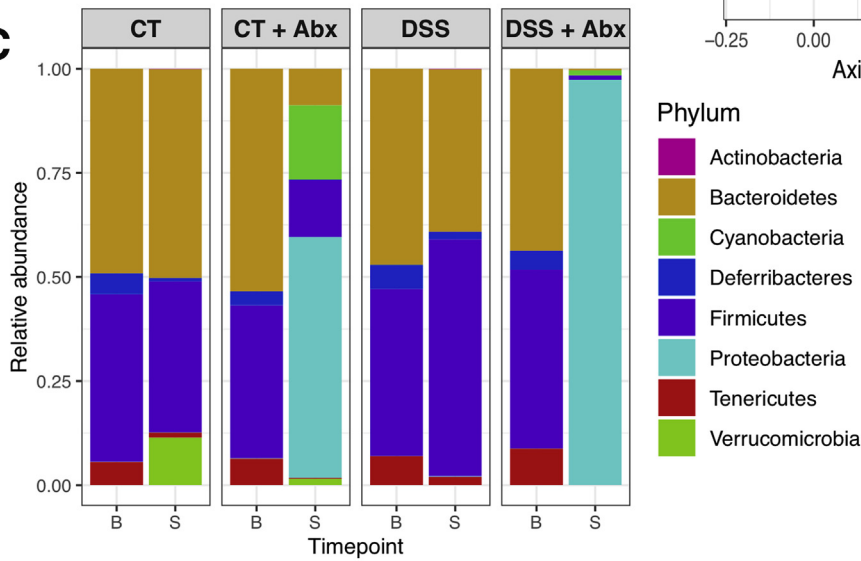
**A**



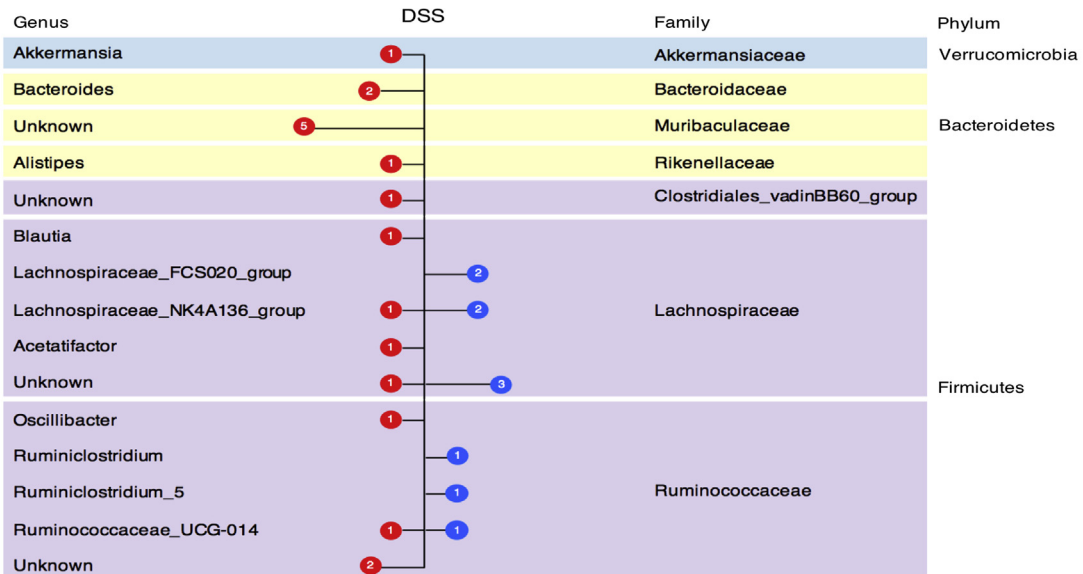
**B**



**C**



**D**



with microbial shifts resulting in an increase in fecal SCFA, in particular butyrate.

### Supernatant From Postinflammatory Dextran Sulfate Sodium Mice Colon Increases Transient Receptor Potential Vanilloid-1 Receptor Function in Naive Dorsal Root Ganglion

To evaluate in vitro correlates of nociceptor activation, we assessed the function of cultured mouse dorsal root ganglion (DRG) neurons expressing TRPV1 and transient receptor potential ankyrin-1 receptor (TRPA1) using calcium imaging and examined responses to the TRPV1 agonist, capsaicin, and the TRPA1 agonist, mustard oil.<sup>37-39</sup> We incubated cultured T9-L2 (colonic projecting)<sup>40,41</sup> DRG neurons with sterile-filtered colonic supernatants, derived from a total of 6 mice, 5 weeks after DSS or control administration (Figure 1A). Thus, we exposed naive TRP-expressing DRG neurons to the nociceptive mediators present in the colon.<sup>39</sup> TRPV1 responses to 100 nmol/L capsaicin stimulation were significantly increased in naive colonic DRGs incubated with colonic supernatant derived from postinflammatory DSS mice compared with controls (area under the curve capsaicin 100 nmol/L: control, 202.4 ± 15.9 vs DSS, 309.8 ± 26.5;  $P < .05$ ) (Figure 8A). In contrast, TRPA1 responses to mustard oil were not different between groups (Figure 8B). We also evaluated responses to capsaicin and mustard oil in hind paw projecting<sup>42</sup> L4-L5 DRG neurons from postinflammatory DSS mice. TRPV1 responses in L4-L5 DRGs from DSS and DSS + Abx treated mice were significantly increased in response to 100 nmol/L capsaicin compared with control mice (area under the curve capsaicin 100 nmol/L: control, 99.5 ± 9.2 vs DSS, 133.4 ± 16.1; control, 99.5 ± 9.2 vs DSS + Abx, 128.5 ± 6.7;  $P < .05$ ) (Figure 8C). No differences were observed in TRPA1 agonist responses between groups (Figure 8D).

Because fecal butyrate content was significantly elevated in the stool of postinflammatory DSS mice, as well as in recipient mice given postinflammatory DSS stool, we investigated the direct effect of SCFA on TRPV1 sensitization. Naive colonic DRG neurons were incubated with sodium acetate (5 mmol/L), sodium butyrate (1 mmol/L), and sodium propionate (1 mmol/L), and responses to capsaicin were examined. TRPV1 responses were increased in the presence of sodium butyrate and sodium propionate but not sodium acetate (area under the curve capsaicin 100 nmol/L: control, 136.7 ± 5.9 vs butyrate, 174.9 ± 11.2; control, 136.7 ± 5.9 vs propionate, 169 ± 7.2) (Figure 8E) when compared

with media alone, suggesting that microbial-derived soluble mediators modulate TRP sensitization.

## Discussion

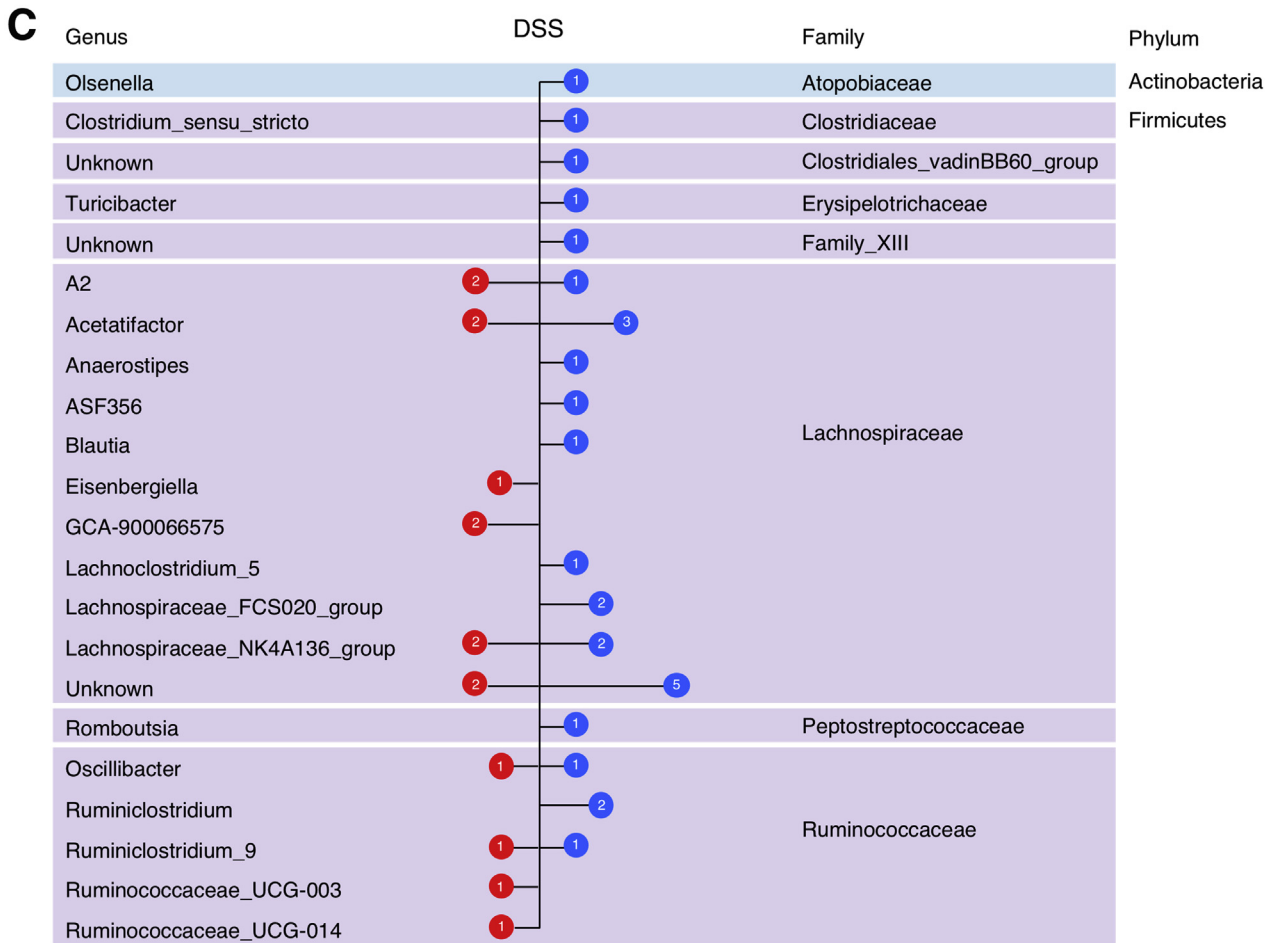
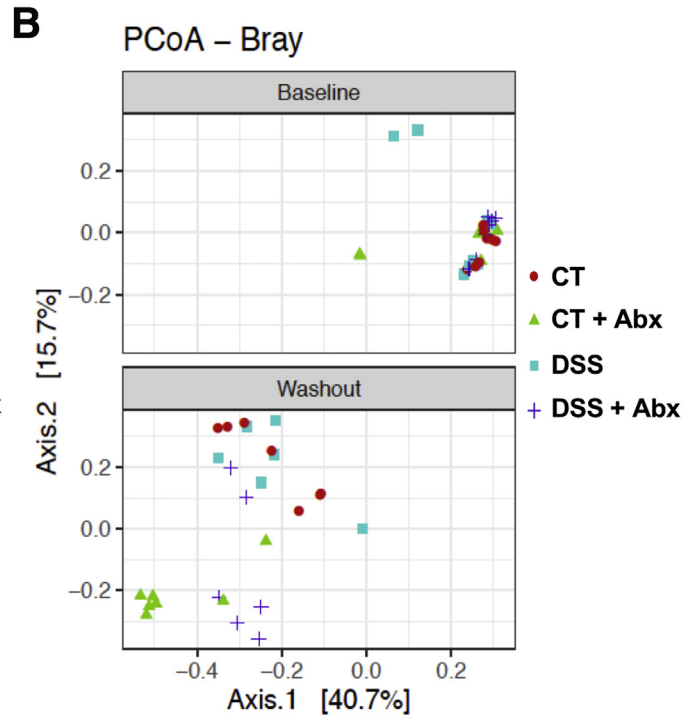
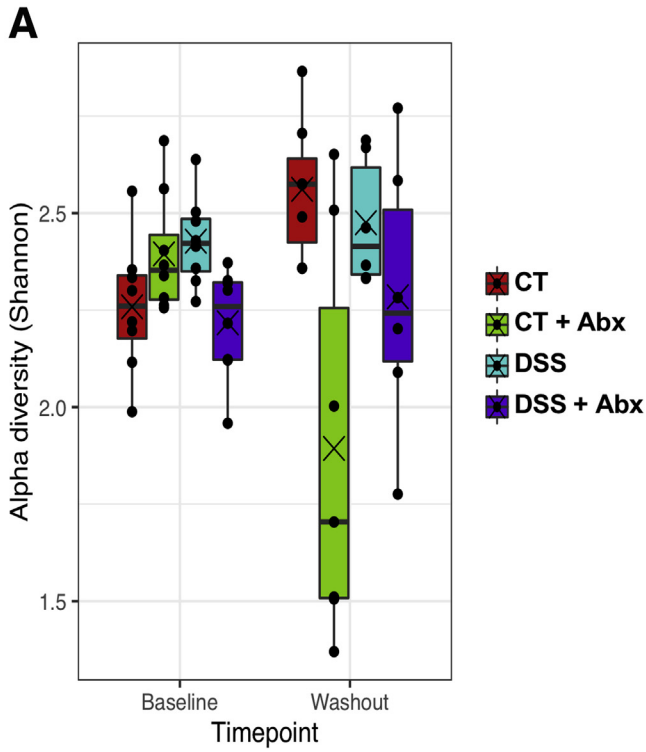
IBD patients in endoscopic remission with chronic abdominal pain display decreased pain thresholds when compared with healthy controls,<sup>43,44</sup> suggesting activation of pro-nociceptive pathways and/or suppression of anti-nociceptive pathways in these patients. It is well-known that the gut microbiome plays a key role in the pathogenesis of IBD<sup>8</sup>; however, the role of the microbiome in the development of chronic visceral pain in IBD is poorly understood. We have demonstrated that microbial manipulation, through the use of Abx or FMT in the postinflammatory DSS mouse, modulates the development of visceral, but not somatic, pain. SCFA-producing species and fecal SCFA content were increased in postinflammatory DSS mice, whereas incubation of cultured DRG neurons with SFCAs in vitro leads to sensitization of TRPV1, suggesting that microbial-derived soluble products such as SCFA are able to sensitize nociceptive neurons.

Chronic visceral pain is a disorder of the gut-brain axis, and both central and peripheral mechanisms contribute to its pathogenesis.<sup>3</sup> Painful sensation from the gut is relayed to the central nervous system by polymodal nociceptors, which transduce mechanical and chemical stimuli.<sup>45</sup> TRPV1 is expressed on a subset of nociceptive peptidergic neurons and transduces inflammatory injury.<sup>45</sup> TRPV1 stimulation has been shown to participate in the generation of neuropathic pain in IBD by provoking the release of neuropeptides such as substance P and calcitonin gene-related peptide from peripheral terminals.<sup>26,46</sup> In conjunction with other inflammatory mediators released during injury or infection, neuropeptides have immunoregulatory properties and can in turn increase nociceptor excitability.<sup>45,46</sup> Thus, TRPV1 sensitization is instrumental in the generation of inflammatory hyperalgesia, or exaggerated pain responses, and allodynia, or pain caused by innocuous stimuli.<sup>45</sup> Furthermore, TRPV1 expression is increased in both patients with acute flares of IBD and experimental models of acute colitis,<sup>26,47</sup> as well as in IBD patients with chronic abdominal pain and endoscopic remission.<sup>15</sup> Because of the pivotal importance of TRPV1 in pain in IBD, we chose to use the postinflammatory DSS mouse model where TRPV1 sensitization was shown to play a crucial role in the generation of chronic postinflammatory visceral pain.<sup>24</sup>

We found that in vitro incubation of naive cultured T9-L2 DRG neurons (colonic projecting<sup>40,41</sup>) with

**Figure 4.** (See previous page). Postinflammatory DSS mice exhibit changes in the microbiome. The alpha (A) and beta (B) diversity was assessed in controls, postinflammatory DSS, and antibiotic-treated mice. Baseline samples were not different; antibiotic treatment caused significant shifts in both alpha (linear mixed-effects model,  $P = .0072$ ) and beta diversity (permutational multivariate analysis of variance,  $P < .001$ ). Points represent individual samples, lines represent the median, and crosses represent the mean. (C) Relative abundance of different phyla at baseline (B) and sacrifice (S) time points. No significantly different phyla were seen at baseline between groups. (D) Comparison of bacterial content at the genus level between control and postinflammatory DSS mice at the sacrifice time point. Blue symbols represent families significantly increased in the postinflammatory DSS mice, and red symbols represent families significantly increased in controls (beta-binomial regression model,  $P < .01$ ). N = 6/group, except DSS + Abx baseline, n = 7, control baseline, n = 5, and DSS + Abx group at sacrifice, n = 4. Abx, antibiotics; DSS, dextran sulfate sodium.





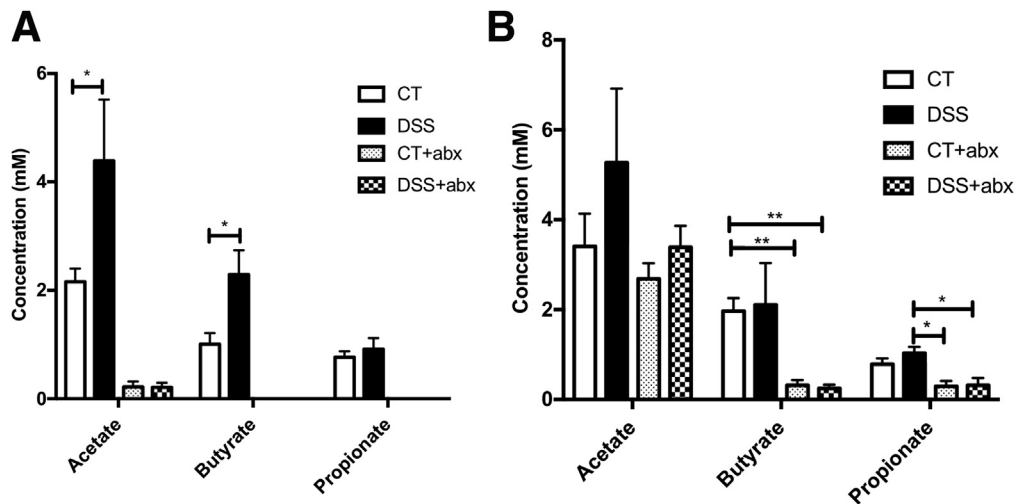


**Figure 6. Postinflammatory DSS mice exhibit elevated stool short-chain fatty acids.** (A) Stool short-chain fatty acid content in postinflammatory DSS mice and controls. In antibiotic-treated animals (Abx), short-chain fatty acid concentration was below the limit of detection for butyrate and propionate. N = 6/group. (B) Stool short-chain fatty acid content after 2 weeks of antibiotic washout. CT and CT + Abx: n = 7, DSS and DSS + Abx: n = 6. One-way analysis of variance: \* $P < .05$ ; \*\* $P < .01$ . Abx, antibiotics; CT, control; DSS, dextran sulfate sodium.

supernatants from postinflammatory DSS mice, but not supernatants from Abx-treated animals, resulted in increased intracellular calcium in response to TRPV1 stimulation with capsaicin. Furthermore, stimulation of L4-L5 DRGs (hind paw projecting<sup>42</sup>) derived directly from postinflammatory DSS mice with capsaicin also resulted in increased intracellular calcium responses when compared with neurons derived from Abx-treated mice alone. This parallels our in vivo data where previous inflammation resulted in somatic and visceral pain. Abx treatment induced visceral hyperalgesia alone; this effect was reversed by a 2-week antibiotic washout period. These data suggest that Abx treatment and previous inflammation cause visceral hyperalgesia through different mechanisms. It should be noted that we did not use retrograde tracers to specifically evaluate colonic projecting neurons, because this technique requires additional surgery/anesthesia and adds increased stress to mice, which itself could lead to visceral pain.<sup>48,49</sup> Previous studies have demonstrated that incubation of naive cultured T9-L2 DRG neurons with sterile-filtered colonic supernatants results in similar findings to direct assessment of colonic projecting neurons.<sup>50</sup>

Postinflammatory DSS mice exhibited somatic as well as visceral hyperalgesia, demonstrating both mechanical and thermal hyperalgesia in our model. This was not affected by Abx treatment. Similarly, FMT of postinflammatory DSS

stool did not result in the transfer of somatic hyperalgesia when compared with control stool or vehicle, suggesting that microbial manipulation does not modulate somatic hyperalgesia. Instead, our data support the idea that the somatic hyperalgesia in our model results from the initial inflammatory insult and is maintained centrally. There is evidence that somatic hyperalgesia results from central sensitization in visceral pain models.<sup>22,25,51-53</sup> For example, mice given DSS for 7 days were shown to display increased neuronal activation in the spinal cord, thalamus, hypothalamus, amygdala, and prefrontal cortex in a previous study.<sup>54</sup> This was associated with mechanical and thermal hyperalgesia of the plantar skin in mice, suggesting that acute colitis caused central sensitization, which then resulted in somatic hyperalgesia.<sup>54</sup> In another study of postinflammatory DSS mice, capsaicin instillation in the colon caused neuronal activation in the dorsal horn, which correlated with somatic hyperalgesia of the abdominal wall, suggesting that in the postinflammatory model, referred somatic pain was secondary to central sensitization.<sup>25</sup> A study in rats demonstrated that broad-spectrum Abx use did not result in thermal hyperalgesia,<sup>22</sup> similar to our own data. Conversely, chemotherapy-induced mechanical hyperalgesia was reduced in Abx-treated as well as germ-free mice.<sup>55</sup> In another study that examined somatic hyperalgesia, broad-spectrum Abx treatment alone resulted

**Figure 5. (See previous page). Postinflammatory DSS mice exhibit persistent changes in the microbiome.** The alpha (A) and beta (B) diversity was assessed in controls, postinflammatory DSS, and mice given antibiotics and then allowed a 2-week washout period. Baseline samples were not different; antibiotic washout allowed some degree of microbial recovery, although there was still a significant difference in the alpha diversity when comparing CT vs CT + Abx groups (Tukey honestly significant difference;  $P = .0067$ ) and in beta diversity when comparing CT vs CT + Abx groups and DSS vs DSS + Abx groups (permutational multivariate analysis of variance, CT vs CT + Abx,  $P = .001$ ; DSS vs DSS + Abx,  $P = .003$ ). Points represent individual samples, lines represent the median, and crosses represent the mean. (C) Comparison of bacterial content at the genus level between control and postinflammatory DSS mice at the washout time point. Blue symbols represent families significantly increased in the post-inflammatory DSS mice, and red symbols represent families significantly increased in controls (beta-binomial regression model,  $P < .01$ ). N = 6-8/group. Abx, antibiotics; CT, control; DSS, dextran sulfate sodium.

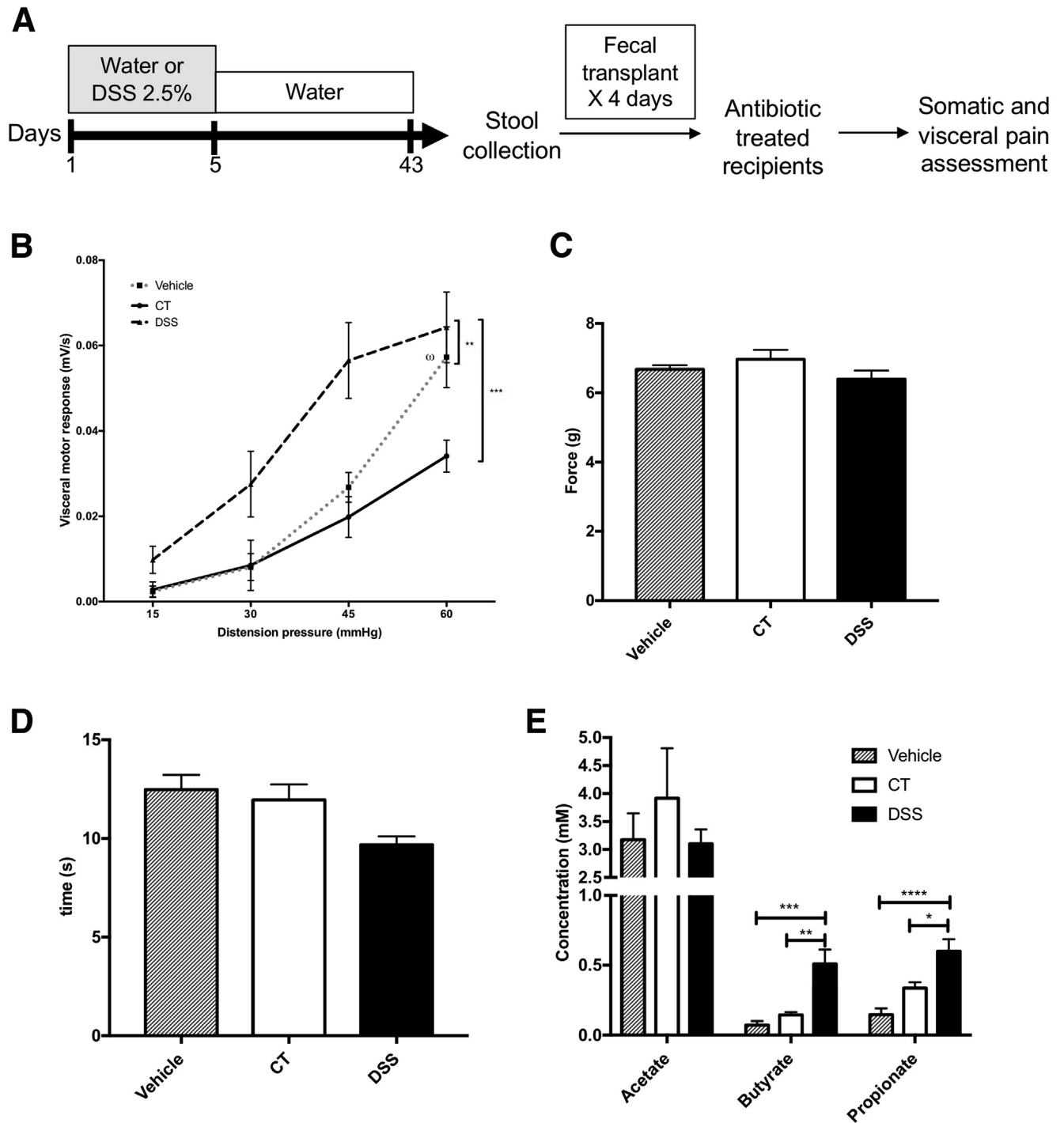
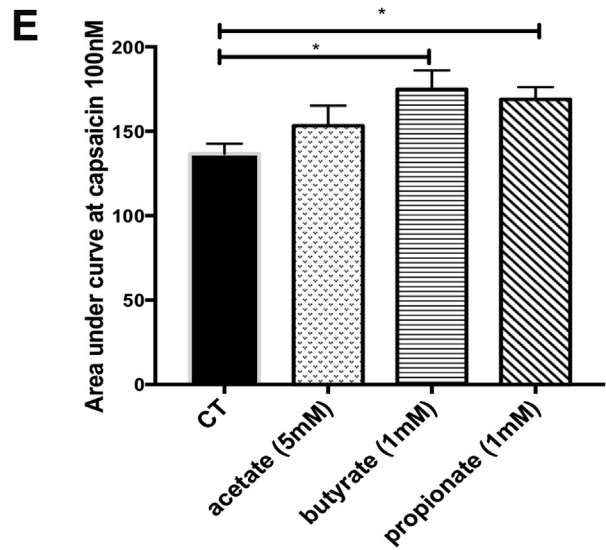
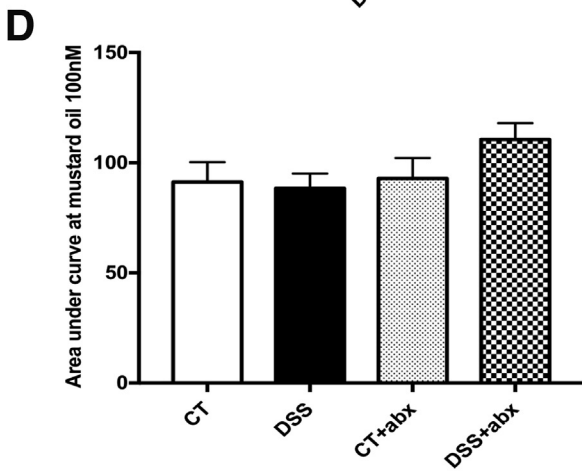
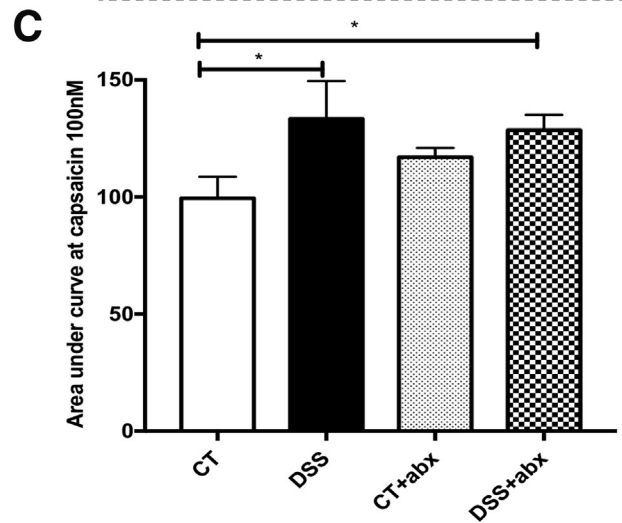
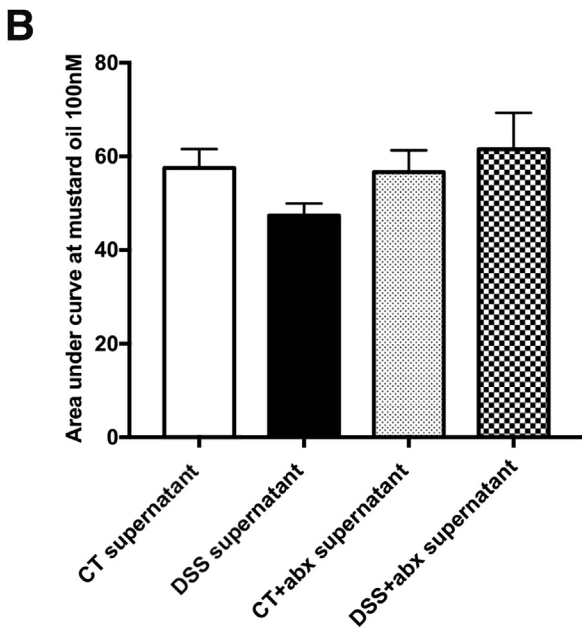
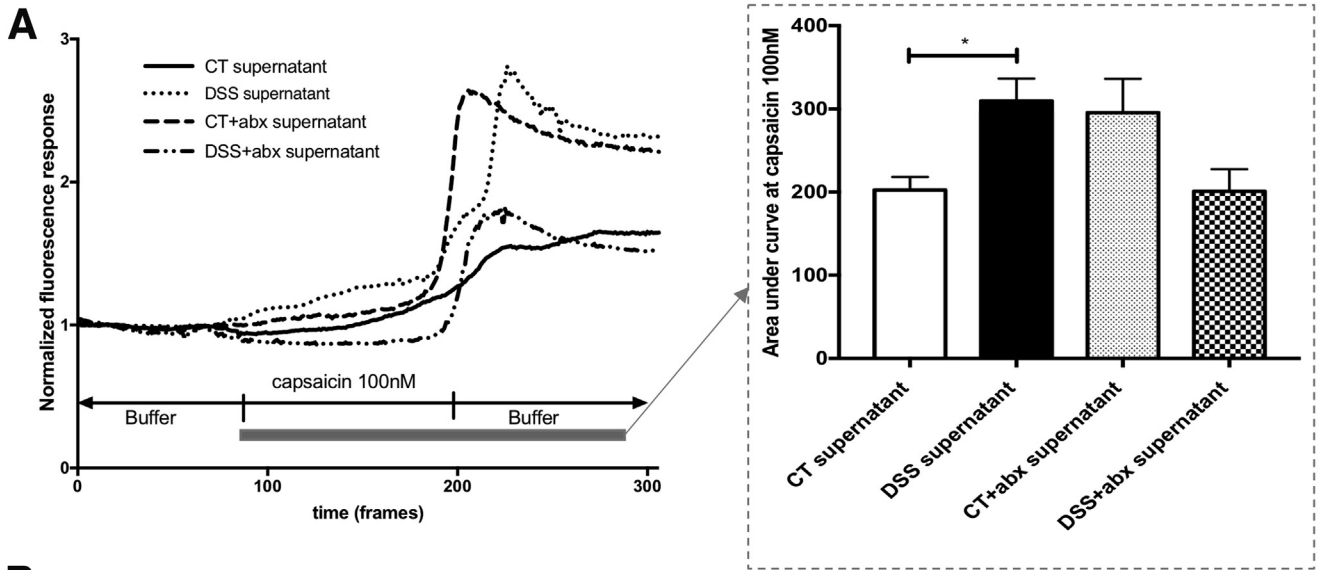


**Figure 7. Fecal microbial transplant of postinflammatory DSS stool transfers the phenotype of visceral but not somatic pain and is associated with increased stool short-chain fatty acids.** (A) Experimental protocol. Antibiotic-treated recipient animals received stool via gavage from postinflammatory DSS mice, controls (CT), or vehicle (sterile phosphate-buffered saline + glycerol) alone. (B) Visceral pain was increased in mice given postinflammatory DSS stool when compared with control and vehicle. Vehicle:  $n = 10$ , CT:  $n = 7$ , DSS:  $n = 11$ , 2 experiments. One-way analysis of variance of area under the curve:  $**P < .01$ ;  $***P < .001$ . Mice given vehicle displayed hyperalgesia at 60 mm Hg compared with mice given control stool (two-way analysis of variance,  $^{\circ}P < .05$ ). Somatic pain, assessed by using automated Von Frey (C) and hot plate tests (D), was unaffected after fecal microbial transplant. Vehicle:  $n = 9$ , CT:  $n = 7$ , DSS:  $n = 8$ , 2 experiments. (E) Fecal butyrate and propionate are increased in the stool of recipient mice given stool from postinflammatory DSS animals when compared with those that received stool from controls or vehicle. Vehicle:  $n = 12$ , CT:  $n = 7$ , DSS:  $n = 11$ .  $**P < .01$ ;  $***P < .001$ ;  $****P < .0001$ . DSS, dextran sulfate sodium.



in mechanical hyperalgesia to the von Frey hair test and the tail-flick test in rats.<sup>56</sup> Taken together, these data suggest that although central sensitization may underlie somatic pain in the postinflammatory state, any role of the microbiome in this phenomenon needs to be examined more closely.

It was striking that Abx treatment alone results in profound visceral hyperalgesia. Metronidazole and neomycin in particular are known to have neurotoxic and ototoxic effects<sup>57–59</sup>; however, visceromotor responses were unchanged after direct catheter infusion of Abx vs vehicle, suggesting that responses in Abx-treated animals were not solely due to neurotoxicity. Previous studies of Abx-treated animals have also found increased visceral pain after Abx treatment. In a seminal study where mice were treated with a 10-day course of oral Abx, animals developed hyperalgesia to colorectal distention, which was associated with increased colonic substance P expression.<sup>31</sup> In a study where neonatal mice were treated with 10 days of Abx, animals developed persistent visceral pain at 10 weeks of age.<sup>60</sup> Interestingly, this was associated with decreased TRPV1 expression in the lumbosacral spinal cord; no evidence of inflammation was seen.<sup>60</sup> Conversely, when adult mice were treated with 6 weeks of broad-spectrum Abx, visceral pain to colorectal distention was markedly attenuated, and this was also associated with decreased TRPV1 expression in the lumbosacral spinal cord.<sup>22</sup> Consistent with these data, germ-free mice displayed visceral hyperalgesia to colorectal distention, an effect that was reversed by bacterial colonization; TRPV1 expression was unchanged in this model.<sup>61</sup> Together, these data suggest that commensal microbes may be anti-nociceptive; Abx treatment or absence of the microbiome seems to abrogate these anti-nociceptive effects. Indeed, probiotics, such as *Lactobacillus* and *Bifidobacterium* species, have been shown to decrease the visceromotor response to colorectal distention in animal models<sup>31,62</sup>; the probiotic *Lactobacillus reuteri* DSM 17938 was able to decrease the capsaicin-induced increase in intracellular calcium in rat DRG neurons and reduce the response of distention evoked firing of spinal nerves, an effect that was abolished in TRPV1 knockout mice.<sup>63</sup> *Faecalibacterium prausnitzii*, a butyrate-producing member of the Firmicutes phyla, was found to decrease the excitability of DRG neurons through a protease-dependent mechanism.<sup>19</sup> In the current study, we observed that Abx-induced visceral hypersensitivity and dysbiosis were independent of SCFAs, whereas microbial shifts in the postinflammatory DSS model and subsequent visceral hypersensitivity were

dependent on SCFA and TRPV1 sensitization. Thus, it is possible that Abx treatment results in dysbiosis and the loss of anti-nociceptive species/soluble mediators, resulting in visceral hyperalgesia.

Postinflammatory DSS mice exhibited microbial shifts in our study, with a relative decrease in Bacteroidetes and an increase in the Firmicutes phyla; close examination at the genus level revealed a relative increase in SCFA-producing species such as *Lachnospiraceae* and *Ruminococcus*. SCFAs such as butyrate are a crucial source of energy for colonocytes and are important in maintaining gut barrier integrity and inhibiting inflammation.<sup>20,64</sup> Our data are in agreement with a previous study that examined the microbiota after 3 cycles of DSS in mice, which also found an increase in *Lachnospiraceae* species.<sup>34</sup> The increase in SCFA-producing Firmicutes is in marked contrast to the microbial profile of patients with active IBD,<sup>9,65–67</sup> where a loss of these SCFA-producing species is more common. However, some patients with irritable bowel syndrome (IBS), a disorder of the brain-gut axis characterized by abdominal pain and altered bowel habits in the absence of overt inflammation,<sup>68</sup> exhibit a similar increase in SCFA-producing species, in particular *Lachnospiraceae*,<sup>69,70</sup> although this finding has not been universal, likely because of the heterogeneous nature of IBS.<sup>71</sup> Interestingly, increased *Lachnospiraceae* species have been noted in the microbiota derived from the stool of both adults<sup>72–74</sup> and children with IBS,<sup>75</sup> and this increase was correlated with visceral pain<sup>72,75</sup> and the activation of brain regions involved in the processing of painful sensorimotor input,<sup>72</sup> suggestive of a causal relationship between this family of bacteria and visceral pain.

In our study, incubation of cultured naive DRG neurons with the SCFAs butyrate and propionate resulted in TRPV1 sensitization, whereas FMT of postinflammatory DSS stool resulted in a further increase in visceral hyperalgesia when compared with Abx alone. This suggests that in the postinflammatory DSS model, the microbiome may be pro-nociceptive. It should be noted that colonic supernatants contain soluble factors derived from both the host and the microbiota; hence, we performed experiments where naive DRG neurons were incubated with SCFA alone. This SCFA concentration was chosen on the basis of the quantification data from mouse stool. The evaluation of fecal SCFA levels is well-described<sup>76–79</sup>; however, it should be noted that fecal/luminal SCFA concentration reflects a dynamic balance between SCFA production and absorption and may not necessarily reflect the true SCFA concentration at the mucosal barrier.<sup>80,81</sup> As such, these levels should be

**Figure 8.** (See previous page). SCFAs modulate TRPV1 sensitization in dorsal root ganglia (DRGs) neurons. T9-L2 DRGs from naive mice (n = 6/group) were cultured overnight with supernatants from CT, Abx-treated, and DSS-treated mice. Cells were stimulated with the TRPV1 (A) or TRPA1 (B) agonists, capsaicin (100 nmol/L) or mustard oil (100 nmol/L), respectively, and calcium imaging was used to evaluate TRPV1 or TRPA1 sensitization. L4-L5 DRGs from postinflammatory mice (n = 6/group) were cultured overnight. (C) Capsaicin (100 nmol/L) or (D) mustard oil (100 nmol/L) was used to evaluate TRPV1 or TRPA1 sensitization using calcium imaging. (E) T9-L2 dorsal root ganglia (n = 6/group) were incubated directly with the short-chain fatty acids acetate (5 mmol/L), butyrate (1 mmol/L), or propionate (1 mmol/L). Cells were stimulated with capsaicin (100 nmol/L), and calcium imaging was used to evaluate TRPV1 sensitization. One-way analysis of variance of area under the curve, \*P < .05 (3 experiments). Abx, antibiotics; CT, control; DSS, dextran sulfate sodium; TRPA1, transient receptor potential ankyrin-1 receptor; TRPV1, transient receptor potential vanilloid-1 receptor.

interpreted with caution. To date, there have been conflicting findings on the role of SCFAs, and in particular butyrate, in visceral pain. Our findings are in agreement with previous data from a rat model where butyrate enemas induced visceral hypersensitivity in control rats through activation of a mitogen-activated protein kinase-dependent mechanism in DRG neurons.<sup>82</sup> Interestingly, in a rat model of acute colitis, butyrate enemas prolonged the nociceptive effect of acute colitis on visceral pain.<sup>83</sup> Furthermore, use of the low fermentable oligosaccharides, disaccharides, monosaccharides, and polyols (low FODMAP) diet, which is effective for the treatment of abdominal pain in IBD patients in remission, results in decreased fecal SCFA content.<sup>77</sup> In contrast with our data, butyrate enemas in healthy patients and mouse models caused a dose-dependent reduction of abdominal pain to colorectal distention.<sup>33,84</sup> Other studies that used Abx to modulate the microbiome, including our own, demonstrate a decrease in fecal butyrate content associated with an increase in pain behaviors,<sup>22,85,86</sup> suggesting that although butyrate may be pro-nociceptive in some model systems, broad-spectrum Abx treatment results in a nonspecific loss in anti-nociceptive bacteria/soluble mediator(s). SCFAs exert their actions through both receptor-mediated and receptor-independent mechanisms.<sup>64</sup> Future pharmacologic and genetic studies should focus on the mechanism whereby SCFAs cause nociceptor sensitization in postinflammatory DSS mice, which will in turn shed light on some of the conflicting data in the literature.

In conclusion, we have demonstrated that the microbiome appears to play an important role in post-inflammatory visceral, but not somatic, hypersensitivity. Microbial-derived soluble products, including sodium butyrate and sodium propionate, were able to sensitize nociceptive neurons *in vitro*, suggesting that these SCFAs may play a role in the pathogenesis of postinflammatory visceral pain.

## Materials and Methods

### Animals

Six-week-old male C57BL/6 mice were obtained from Charles River Laboratories (Montreal, Quebec, Canada). All mice were housed in plastic sawdust floor cages under standard conditions with free access to drinking water and food. All experiments were conducted on age-matched animals under protocols approved by the University of Calgary Animal Care Committee and in accordance with the guidelines for the ethical use of animals in research of the Canadian Council on Animal Care (AC16-0105). All animals were allowed to acclimatize for 1 week before any experimentation.

### Induction of Inflammation and Microbial Manipulation

Colonic inflammation was induced by administration of 2.5% (wt/vol) DSS (36,000–50,000 MW; MP Biochemicals, Solon, OH) in drinking water for 5 days. Mice were separated into 2 groups, control untreated and DSS treated, and

were allowed to recover for 5 weeks before the evaluation of visceral hyperalgesia.<sup>24</sup> To manipulate the microbiome, mice received an Abx cocktail consisting of ampicillin, neomycin, metronidazole (1 g/L), and vancomycin (0.5 g/L)<sup>31,60</sup> (all from Sigma-Aldrich Canada, Oakville, ON, Canada) administered in drinking water 2 weeks before the end of the recovery period. In some cases, mice were allowed to recover for a further 2 weeks after the discontinuation of Abx. Weight changes were measured daily in all mice. Colonic length and thickness were assessed at the time of death as previously described.<sup>24</sup>

Microbial manipulation was also performed by using FMT. Fresh fecal pellets from 6 donor mice were collected, pooled, and weighed. Pellets were homogenized for 5 minutes in 1 mL sterilized PBS supplemented with 10% glycerol by using 1 mm zirconium oxide beads (NextAdvance, Troy, NY) in a 4°C cold room using a bullet blender (NextAdvance). The volume was adjusted to give a concentration of 80 mg feces/mL. The fecal matter was centrifuged for 1 minute at 400g, and the supernatant was used for FMT. Recipient mice were pretreated with the previously described Abx cocktail to disrupt the basal microbiome. Subsequently, Abx-treated mice received 80 mg/mL homogenized stool in 200  $\mu$ L sterile saline + 10% glycerol or sterile saline + 10% glycerol alone for 4 days via orogastric gavage.<sup>29,30</sup>

### *In Vivo Measurement of Somatic and Visceral Pain*

**Visceromotor response to colorectal distention.** The visceromotor response to colorectal distention was assessed as previously described.<sup>24</sup> Briefly, 2 days before colorectal distention, mice were anesthetized with xylazine and ketamine, and electrodes were implanted bilaterally into the abdominal external oblique musculature (Bioflex AS-631; Cooner Wire, Chatsworth, CA). Electrodes were exteriorized at the back of the neck and protected by a plastic tube attached to the skin. Mice were allowed to recover for 48 hours after electrode implantation. For recording, electrodes were connected to a Bio Amplifier, which was then connected to an electromyogram acquisition system (both from ADInstruments, Colorado Springs, CO). A 10.5-mm-diameter balloon catheter (Fogarty arterial embolectomy catheter, 4F; Vygon USA, Lansdale, PA) was gently inserted into the rectum to a depth of 5 mm. Ten-second distentions were performed at pressures of 15, 30, 45, and 60 mm Hg by inflating the balloon in a stepwise fashion with water (20, 40, 60 and 80  $\mu$ L, respectively) with 5-minute rest intervals. The electromyographic activity of the abdominal muscles was recorded, and visceromotor responses were calculated by using LabChart 7 software (ADInstruments).

To evaluate whether Abx exerted direct effects on visceral sensitivity, Abx or sterile saline (vehicle) were administered directly into the colon via a double lumen catheter, similar to a previous study.<sup>31</sup> Visceromotor responses were tested before and 1 hour after administration of saline or Abx.

**Somatic pain assessment.** Somatic pain evaluation was performed by a blinded investigator. Mechanical and thermal sensitivities were tested simultaneously in all groups on the same day.

**Mechanical sensitivity.** Mechanical sensitivity was tested by measuring the threshold to withdrawal applied to the paw using the automated Von Frey hair test (Ugo Basile, Gemonio, Italy) as described.<sup>87</sup> Mice were individually placed in custom-made plastic compartments on a metallic mesh for 1 hour, 2 days before testing, to minimize stress reactions. On the day of the experiment, 8 mice were allowed to habituate in individual opaque compartments until exploratory behavior was no longer observed (~20–30 minutes). The hind paw withdrawal threshold was measured by applying a small metal filament that automatically exerts constant progressive pressure perpendicular to the middle of the plantar surface of the hind paw until withdrawal. The force and latency values were recorded. This was repeated 5 times, and each trial was followed by a 10-minute resting period. In each animal, the left or right hind paw was chosen at random, and the withdrawal threshold was measured in all animals in a row, followed by evaluation of the opposite hind paw.

**Thermal sensitivity.** Thermal sensitivity was assessed by using the hot plate test<sup>87</sup> (Bioseb, Pinellas Park, FL). Immediately after the automated Von Frey test, mice were placed on a metal hot plate set to  $52^{\circ}\text{C} \pm 0.5^{\circ}\text{C}$ . The latency from placement of the mouse on the heated surface until the first overt behavioral sign of nociception, such as lifting or licking a hind paw, vocalization, or jumping, was measured. The timer was stopped, and the mouse was immediately removed from the hot plate after responding or after a maximum cutoff of 20 seconds to prevent tissue damage.

### ***In Vitro Evaluation of Somatic and Visceral Pain***

**Supernatant generation.** Colonic supernatants were generated as previously described.<sup>37,88</sup> Briefly, full circumference colonic tissue sections of 5 mm from all mice used for somatic and visceral pain experiments were transferred and incubated for 1 hour in 96-well plate containing 300  $\mu\text{L}$  Hanks' balanced salt solution (HBSS) supplemented with calcium chloride and magnesium chloride (Gibco, Carlsbad, CA) in a humidified incubator at  $37^{\circ}\text{C}$  under 95% air and 5%  $\text{CO}_2$ ; samples were not standardized to the weight of segments. Supernatants were filtered (0.2  $\mu\text{m}$  pore polyethersulfone membrane) and stored at  $-80^{\circ}\text{C}$ . For in vitro experiments involving calcium imaging, pooled supernatants derived from mice in the same treatment group were used. Pooled supernatants from 2 animals of the appropriate treatment group were used for calcium imaging for each experiment, where naive DRGs were imaged from 2 mice at a time. Three total experiments were performed; naive DRGs from a total of 6 mice were used for the calcium imaging. These DRGs were incubated with pooled supernatants derived from a total of 6 different animals from the appropriate treatment group.

### ***Dorsal Root Ganglion Dissection and Culture***

Culture of isolated DRG neurons was performed as previously described.<sup>24,37</sup> Mice were killed by an overdose of ketamine and xylazine, followed by cervical transection. The spinal cord was removed, and the DRGs from T9 to L2 were dissected and removed, because these levels receive nociceptive input from the colon.<sup>40,41</sup> For assessment of somatic nociceptive input, L4-L5 DRGs, which receive nociceptive input from the hind paw,<sup>42</sup> were dissected. Isolated DRGs were incubated at  $37^{\circ}\text{C}$  in HBSS containing 5100 U/mL Type 1 collagenase (Gibco) and 7.1 U/mL dispase II (Roche, Mannheim, Germany). DRGs were washed in Dulbecco modified Eagle medium (DMEM) (Gibco) containing 10% fetal calf serum, and ganglia were then triturated with a fire-polished Pasteur pipette. Dispersed neurons were suspended in 1 mL DMEM containing 10% fetal bovine serum, 1% penicillin/streptomycin, and 100 ng/mL nerve growth factor (Corning, Tewksbury, MA). The cell suspension was plated onto laminin-coated coverslips (Corning) and stored in a humidified incubator at  $37^{\circ}\text{C}$  under 95% air and 5%  $\text{CO}_2$ . After 3 hours, the medium was replaced. For experiments involving colonic supernatants, cells were pretreated overnight with 500  $\mu\text{L}$  supernatant (diluted  $1/2$  in DMEM containing 10% fetal bovine serum and 1% penicillin/streptomycin); supernatants from 2 mice within the same group were pooled for each experiment as described above. For experiments involving SCFAs, sodium acetate (5 mmol/L), sodium butyrate (1 mmol/L), and sodium propionate (1 mmol/L) (all from Sigma) were diluted in DMEM and incubated overnight with cultured DRGs. The pH of the medium was not significantly altered in the presence of these SCFAs (pH 7.3–7.5).

### ***Calcium Imaging***

Calcium imaging was performed as previously described.<sup>39</sup> Cultured DRGs were imaged by using a  $10\times$  objective on an Olympus IX51 microscope controlled by cellSens software (Olympus Canada, Toronto, ON, Canada). Cultured DRG neurons were loaded in HBSS (Gibco) with 2  $\mu\text{mol/L}$  Fura-2AM (Life Technologies, Carlsbad, CA) for 30 minutes at  $37^{\circ}\text{C}$  and then washed with HBSS for 20 minutes at  $37^{\circ}\text{C}$ . The recording chamber was continually perfused at  $37^{\circ}\text{C}$  with external solution (in mmol/L: 140 NaCl, 5 KCl, 10 HEPES, 10 glucose, 1  $\text{MgCl}_2$ , 2  $\text{CaCl}_2$ ; pH adjusted to 7.3–7.4 with 10N NaOH). To examine TRPV1 or TRPA1 activity, cells were perfused with doses of the TRPV1 agonist capsaicin (100 nmol/L and 1  $\mu\text{mol/L}$ ; Sigma) or the TRPA1 agonist mustard oil (100 nmol/L and 1  $\mu\text{mol/L}$ ; Sigma) diluted in external solution at a rate of  $\sim 1$  mL/min. Fluorescence was measured during excitation at 340 and 380 nm, and the ratio of the fluorescence emission at 510 nm was monitored. The baseline was monitored for 120 seconds before perfusion with agonist. Images were acquired every 1 second and processed by using ImageJ (NIH, Bethesda, MD) by drawing discrete regions of interest around cells that responded to KCl (70 mmol/L). Data are expressed as a fold change from baseline fluorescence normalized to background

fluorescence ( $\Delta F/F_0$ ) on raw traces and were analyzed by using area under the curve.

### Microbial Sequencing and Metabolomic Data

**16S rRNA gene amplicon sequencing.** DNA extraction and purification from feces were performed by using QIAamp Fast DNA Stool extraction kit (Qiagen, Toronto, ON, Canada). The V4 hypervariable region of the 16S rRNA gene was amplified by using the following barcoded primers with MiSeq (Illumina, San Diego, CA) -specific adaptors: 16SV4Fwd: AATGATACGGCGACCACCGAGATCTACACBARCODETATGGTAATTGT GTGCCAGCMGCCGCGGTAA and 16SV4Rev: CAAGCAGAAGACGGCATACGAGAT BARCODEAGTCAGTCAGCCGGACTACHVGGGTWTCTAAT. KAPA HiFi polymerase (Roche) was used under the following cycling conditions: initial denaturation 98°C for 2 minutes, 25 cycles of 98°C for 30 seconds, 55°C for 30 seconds, 72°C for 20 seconds, and final elongation at 72°C for 7 minutes. NucleoMag NGS (Macherey-Nagel, Bethlehem, PA) was used for polymerase chain reaction (PCR) cleanup and size selection, followed by PCR product normalization with the SequalPrep Normalization Plate Kit (ThermoFisher, Waltham, MA) according to the manufacturer's protocols. Individual PCR libraries were pooled and then qualitatively and quantitatively assessed on a High Sensitivity D1000 ScreenTape station (Agilent, Waldbronn, Germany) and on a Qubit fluorometer (ThermoFisher). The 16S rRNA v4 gene amplicon sequencing was performed by using a V2-500 cycle cartridge (Illumina) on the MiSeq platform (Illumina).

Raw fastq files were processed by using Cutadapt (version 1.16<sup>89</sup>) and dada2 (R package, version 1.10.1<sup>90</sup>). After removing standard Illumina V4 primers and reads shorter than 50 base pairs, quality filtering was performed by using the filterAndTrim function of dada2, removing reads with an expected error ( $EE = \sum(10^{-Q}/10)$ ) higher than 2 for both forward and reverse reads. A table of amplicon sequence variants (ASVs) was generated by using the standard dada2 workflow: generating an error model of the data, inferring sequence variants, merging forward and reverse reads, generating a count table, and removing chimeric sequences. Taxonomic classifications were assigned to ASVs by using the dada2::assignTaxonomy function, using the Silva 132 database as a reference.

### Liquid Chromatography–Mass Spectrometry Based Short-Chain Fatty Acids Quantification in Mouse Fecal Samples

Samples were processed and analyzed as previously described.<sup>91</sup> In brief, SCFAs were extracted (1:2 ratio wet sample weight [mg] to extraction solvent [ $\mu$ L]) from fecal samples with ice-cold extraction solvent (50% water/ acetonitrile, v/v) spiked with <sup>13</sup>C-labeled SCFA standards (acetic acid-1,2-<sup>13</sup>C<sub>2</sub>, propionic acid-<sup>13</sup>C<sub>3</sub>, and butyric acid-1,2-<sup>13</sup>C<sub>2</sub>), derivatized with N-(3-dimethylaminopropyl)-N'-ethylcarbodiimide hydrochloride and aniline, and then submitted to liquid chromatography–mass spectrometry analysis. The UHPLC-MS platform consisted of a Vanquish ultrahigh-performance liquid chromatography system

coupled to a TSQ Quantum Access MAX triple quadrupole Mass Spectrometer (Thermo Scientific) equipped with an electrospray ionization probe. In short, SCFAs were separated on a Hypersil GOLD TM C18 column (200 × 2.1 mm, 1.9  $\mu$ m; Thermo Scientific) by using a binary solvent system composed of liquid chromatography–mass spectrometry grade water and methanol, both containing 0.1% (%v/v) formic acid, and monitored with the mass spectrometer operating in positive ionization mode and selected reaction monitoring mode. Data analyses, on the converted mzXML files, were conducted in MAVEN,<sup>92,93</sup> and the absolute quantification of native SCFA concentration was based on the <sup>12</sup>C:<sup>13</sup>C signal intensity ratio and the respective <sup>13</sup>C-internal standard concentration.

### Statistical Analysis

All data are expressed as the mean  $\pm$  standard error of the mean. Treatment effects were analyzed by Student *t* test using Prism 7 (GraphPad, La Jolla, CA). Data distribution was tested by using the D'Agostino and Pearson normality test. One-way or two-way analysis of variance with Bonferroni or Tukey post hoc test was applied for comparison of multiple groups. If the data were found to be not normally distributed, a Kruskal-Wallis test followed by a Dunn multiple comparison or a Mann-Whitney test was used (Prism 7). A *P* value < .05 was considered to be significant. The 16S rRNA sequencing analysis was carried out by using the R package phyloseq (version 1.24.2<sup>94</sup>). Alpha diversity was estimated by using the Shannon index of diversity, and significance was determined by using a mixed-effects linear model, with treatment and time point as fixed effects and mouse ID as a random effect. Beta diversity was estimated by using a principal coordinates analysis on a matrix of Bray-Curtis distances and analyzed by using permutational multivariate analysis of variance. To test for significant differences in composition at the phylum level, a beta-binomial regression model was performed by using the R package corncob. Differential abundance analysis was carried out by using the R package DESeq2<sup>95</sup> to identify ASVs that were differentially abundant across treatments. ASV counts were modeled by using the negative binomial distribution, and significance was determined by a Wald test on log<sub>2</sub> fold change values and an alpha = 0.01. *P* values were adjusted for multiple inference by using the Benjamini-Hochberg method.

### References

1. Molodecky NA, Soon IS, Rabi DM, Ghali WA, Ferris M, Chernoff G, Benchimol EI, Panaccione R, Ghosh S, Barkema HW, Kaplan GG. Increasing incidence and prevalence of the inflammatory bowel diseases with time, based on systematic review. *Gastroenterology* 2012;142:46–54 e42; quiz e30.
2. Gracie DJ, Williams CJ, Sood R, Mumtaz S, Bholah MH, Hamlin PJ, Ford AC. Negative effects on psychological health and quality of life of genuine irritable bowel syndrome-type symptoms in patients with inflammatory



- bowel disease. *Clin Gastroenterol Hepatol* 2017; 15:376–384.
3. Regueiro M, Greer JB, Szigethy E. Etiology and treatment of pain and psychosocial issues in patients with inflammatory bowel diseases. *Gastroenterology* 2017; 152:430–439.
  4. Jonefall B, Ohman L, Simren M, Strid H. IBS-like symptoms in patients with ulcerative colitis in deep remission are associated with increased levels of serum cytokines and poor psychological well-being. *Inflamm Bowel Dis* 2016;22:2630–2640.
  5. Jonefall B, Strid H, Ohman L, Svedlund J, Bergstedt A, Simren M. Characterization of IBS-like symptoms in patients with ulcerative colitis in clinical remission. *Neurogastroenterol Motil* 2013;25, 756–e578.
  6. Buskila D, Odes LR, Neumann L, Odes HS. Fibromyalgia in inflammatory bowel disease. *J Rheumatol* 1999; 26:1167–1171.
  7. Targownik LE, Nugent Z, Singh H, Bugden S, Bernstein CN. The prevalence and predictors of opioid use in inflammatory bowel disease: a population-based analysis. *Am J Gastroenterol* 2014;109:1613–1620.
  8. DeGruttola AK, Low D, Mizoguchi A, Mizoguchi E. Current understanding of dysbiosis in disease in human and animal models. *Inflamm Bowel Dis* 2016;22:1137–1150.
  9. Halfvarson J, Brislawn CJ, Lamendella R, Vazquez-Baeza Y, Walters WA, Bramer LM, D’Amato M, Bonfiglio F, McDonald D, Gonzalez A, McClure EE, Dunklebarger MF, Knight R, Jansson JK. Dynamics of the human gut microbiome in inflammatory bowel disease. *Nat Microbiol* 2017;2:17004.
  10. Shutkever O, Gracie DJ, Young C, Wood HM, Taylor M, John Hamlin P, Ford AC, Quirke P. No significant association between the fecal microbiome and the presence of irritable bowel syndrome-type symptoms in patients with quiescent inflammatory bowel disease. *Inflamm Bowel Dis* 2018;24:1597–1605.
  11. Manichanh C, Rigottier-Gois L, Bonnaud E, Gloux K, Pelletier E, Frangeul L, Nalin R, Jarrin C, Chardon P, Marteau P, Roca J, Dore J. Reduced diversity of faecal microbiota in Crohn’s disease revealed by a metagenomic approach. *Gut* 2006;55:205–211.
  12. Lopez-Siles M, Enrich-Capo N, Aldegue X, Sabat-Mir M, Duncan SH, Garcia-Gil LJ, Martinez-Medina M. Alterations in the abundance and co-occurrence of *Akkermansia muciniphila* and *Faecalibacterium prausnitzii* in the colonic mucosa of inflammatory bowel disease subjects. *Front Cell Infect Microbiol* 2018;8:281.
  13. Martinez C, Antolin M, Santos J, Torrejon A, Casellas F, Borrueal N, Guarner F, Malagelada JR. Unstable composition of the fecal microbiota in ulcerative colitis during clinical remission. *Am J Gastroenterol* 2008; 103:643–648.
  14. Hotte NS, Salim SY, Tso RH, Albert EJ, Bach P, Walker J, Dieleman LA, Fedorak RN, Madsen KL. Patients with inflammatory bowel disease exhibit dysregulated responses to microbial DNA. *PLoS One* 2012;7:e37932.
  15. Akbar A, Yiangou Y, Facer P, Brydon WG, Walters JR, Anand P, Ghosh S. Expression of the TRPV1 receptor differs in quiescent inflammatory bowel disease with or without abdominal pain. *Gut* 2010;59:767–774.
  16. Chiu IM, Heesters BA, Ghasemlou N, Von Hehn CA, Zhao F, Tran J, Wainger B, Strominger A, Muralidharan S, Horswill AR, Bubeck Wardenburg J, Hwang SW, Carroll MC, Woolf CJ. Bacteria activate sensory neurons that modulate pain and inflammation. *Nature* 2013;501:52–57.
  17. Nohr MK, Egerod KL, Christiansen SH, Gille A, Offermanns S, Schwartz TW, Moller M. Expression of the short chain fatty acid receptor GPR41/FFAR3 in autonomic and somatic sensory ganglia. *Neuroscience* 2015; 290:126–137.
  18. Stilling RM, van de Wouw M, Clarke G, Stanton C, Dinan TG, Cryan JF. The neuropharmacology of butyrate: the bread and butter of the microbiota-gut-brain axis? *Neurochem Int* 2016;99:110–132.
  19. Sessenwein JL, Baker CC, Pradhananga S, Maitland ME, Petrof EO, Allen-Vercoe E, Noordhof C, Reed DE, Vanner SJ, Lomax AE. Protease-mediated suppression of DRG neuron excitability by commensal bacteria. *J Neurosci* 2017;37:11758–11768.
  20. Lomax AE, Pradhananga S, Sessenwein JL, O’Malley D. Bacterial modulation of visceral sensation: mediators and mechanisms. *Am J Physiol Gastrointest Liver Physiol* 2019;317:G363–G372.
  21. Meseguer V, Alpizar YA, Luis E, Tajada S, Denlinger B, Fajardo O, Manenschijn JA, Fernandez-Pena C, Talavera A, Kichko T, Navia B, Sanchez A, Senaris R, Reeh P, Perez-Garcia MT, Lopez-Lopez JR, Voets T, Belmonte C, Talavera K, Viana F. TRPA1 channels mediate acute neurogenic inflammation and pain produced by bacterial endotoxins. *Nat Commun* 2014; 5:3125.
  22. Hoban AE, Moloney RD, Golubeva AV, McVey Neufeld KA, O’Sullivan O, Patterson E, Stanton C, Dinan TG, Clarke G, Cryan JF. Behavioural and neurochemical consequences of chronic gut microbiota depletion during adulthood in the rat. *Neuroscience* 2016;339:463–477.
  23. Guida F, Turco F, Iannotta M, De Gregorio D, Palumbo I, Sarnelli G, Furiano A, Napolitano F, Boccella S, Luongo L, Mazzitelli M, Usiello A, De Filippis F, Iannotti FA, Piscitelli F, Ercolini D, de Novellis V, Di Marzo V, Cuomo R, Maione S. Antibiotic-induced microbiota perturbation causes gut endocannabinoid changes, hippocampal neuroglial reorganization and depression in mice. *Brain Behav Immun* 2018; 67:230–245.
  24. Lapointe TK, Basso L, Iftinca MC, Flynn R, Chapman K, Dietrich G, Vergnolle N, Altier C. TRPV1 sensitization mediates postinflammatory visceral pain following acute colitis. *Am J Physiol Gastrointest Liver Physiol* 2015; 309:G87–G99.
  25. Eijkelkamp N, Kavelaars A, Elsenbruch S, Schedlowski M, Holtmann G, Heijnen CJ. Increased visceral sensitivity to capsaicin after DSS-induced colitis in mice: spinal cord c-Fos expression and behavior. *Am J Physiol Gastrointest Liver Physiol* 2007;293:G749–G757.

26. Engel MA, Khalil M, Mueller-Tribbenese SM, Becker C, Neuhuber WL, Neurath MF, Reeh PW. The proximodistal aggravation of colitis depends on substance P released from TRPV1-expressing sensory neurons. *J Gastroenterol* 2012;47:256–265.
27. Palm O, Moum B, Jahnsen J, Gran JT. Fibromyalgia and chronic widespread pain in patients with inflammatory bowel disease: a cross sectional population survey. *J Rheumatol* 2001;28:590–594.
28. Rakoff-Nahoum S, Paglino J, Eslami-Varzaneh F, Edberg S, Medzhitov R. Recognition of commensal microflora by toll-like receptors is required for intestinal homeostasis. *Cell* 2004;118:229–241.
29. Le Bastard Q, Ward T, Sidiropoulos D, Hillmann BM, Chun CL, Sadowsky MJ, Knights D, Montassier E. Fecal microbiota transplantation reverses antibiotic and chemotherapy-induced gut dysbiosis in mice. *Sci Rep* 2018;8:6219.
30. Bromberg JS, Hittle L, Xiong Y, Saxena V, Smyth EM, Li L, Zhang T, Wagner C, Fricke WF, Simon T, Brinkman CC, Mongodin EF. Gut microbiota-dependent modulation of innate immunity and lymph node remodeling affects cardiac allograft outcomes. *JCI Insight* 2018;3.
31. Verdu EF, Bercik P, Verma-Gandhu M, Huang XX, Blennerhassett P, Jackson W, Mao Y, Wang L, Rochat F, Collins SM. Specific probiotic therapy attenuates antibiotic induced visceral hypersensitivity in mice. *Gut* 2006;55:182–190.
32. Amaral FA, Sachs D, Costa VV, Fagundes CT, Cisalpino D, Cunha TM, Ferreira SH, Cunha FQ, Silva TA, Nicoli JR, Vieira LQ, Souza DG, Teixeira MM. Commensal microbiota is fundamental for the development of inflammatory pain. *Proc Natl Acad Sci U S A* 2008;105:2193–2197.
33. Russo R, De Caro C, Avagliano C, Cristiano C, La Rana G, Mattace Raso G, Berni Canani R, Meli R, Calignano A. Sodium butyrate and its synthetic amide derivative modulate nociceptive behaviors in mice. *Pharmacol Res* 2016;103:279–291.
34. Berry D, Kuzyk O, Rauch I, Heider S, Schwab C, Hainzl E, Decker T, Muller M, Strobl B, Schleper C, Urich T, Wagner M, Kenner L, Loy A. Intestinal microbiota signatures associated with inflammation history in mice experiencing recurring colitis. *Front Microbiol* 2015;6:1408.
35. Langille MG, Meehan CJ, Koenig JE, Dhanani AS, Rose RA, Howlett SE, Beiko RG. Microbial shifts in the aging mouse gut. *Microbiome* 2014;2:50.
36. Tachon S, Zhou J, Keenan M, Martin R, Marco ML. The intestinal microbiota in aged mice is modulated by dietary resistant starch and correlated with improvements in host responses. *FEMS Microbiol Ecol* 2013;83:299–309.
37. Guerrero-Alba R, Valdez-Morales EE, Jimenez-Vargas NN, Lopez-Lopez C, Jaramillo-Polanco J, Okamoto T, Nasser Y, Bunnett NW, Lomax AE, Vanner SJ. Stress activates pronociceptive endogenous opioid signalling in DRG neurons during chronic colitis. *Gut* 2017;66:2121–2131.
38. Cattaruzza F, Spreadbury I, Miranda-Morales M, Grady EF, Vanner S, Bunnett NW. Transient receptor potential ankyrin-1 has a major role in mediating visceral pain in mice. *Am J Physiol Gastrointest Liver Physiol* 2010;298:G81–G91.
39. Wouters MM, Balemans D, Van Wanrooy S, Dooley J, Cibert-Goton V, Alpizar YA, Valdez-Morales EE, Nasser Y, Van Veldhoven PP, Vanbrabant W, Van der Merwe S, Mols R, Ghesquiere B, Cirillo C, Kortekaas I, Carmeliet P, Peetermans WE, Vermeire S, Rutgeerts P, Augustijns P, Hellings PW, Belmans A, Vanner S, Bulmer DC, Talavera K, Vanden Berghe P, Liston A, Boeckxstaens GE. Histamine receptor H1-mediated sensitization of TRPV1 mediates visceral hypersensitivity and symptoms in patients with irritable bowel syndrome. *Gastroenterology* 2016;150:875–887 e9.
40. Hockley JRF, Taylor TS, Callejo G, Wilbrey AL, Gutteridge A, Bach K, Winchester WJ, Bulmer DC, McMurray G, Smith ESJ. Single-cell RNAseq reveals seven classes of colonic sensory neuron. *Gut* 2019;68:633–644.
41. Moore BA, Stewart TM, Hill C, Vanner SJ. TNBS ileitis evokes hyperexcitability and changes in ionic membrane properties of nociceptive DRG neurons. *Am J Physiol Gastrointest Liver Physiol* 2002;282:G1045–G1051.
42. da Silva Serra I, Husson Z, Bartlett JD, Smith ES. Characterization of cutaneous and articular sensory neurons. *Mol Pain* 2016;12.
43. van Hoboken EA, Thijssen AY, Verhaaren R, van der Veek PP, Prins FA, Verspaget HW, Masclee AA. Symptoms in patients with ulcerative colitis in remission are associated with visceral hypersensitivity and mast cell activity. *Scand J Gastroenterol* 2011;46:981–987.
44. Faure C, Giguere L. Functional gastrointestinal disorders and visceral hypersensitivity in children and adolescents suffering from Crohn's disease. *Inflamm Bowel Dis* 2008;14:1569–1574.
45. Basso L, Altier C. Transient receptor potential channels in neuropathic pain. *Curr Opin Pharmacol* 2016;32:9–15.
46. Engel MA, Becker C, Reeh PW, Neurath MF. Role of sensory neurons in colitis: increasing evidence for a neuroimmune link in the gut. *Inflamm Bowel Dis* 2011;17:1030–1033.
47. Yiangou Y, Facer P, Dyer NH, Chan CL, Knowles C, Williams NS, Anand P. Vanilloid receptor 1 immunoreactivity in inflamed human bowel. *Lancet* 2001;357:1338–1339.
48. Zheng G, Hong S, Hayes JM, Wiley JW. Chronic stress and peripheral pain: evidence for distinct, region-specific changes in visceral and somatosensory pain regulatory pathways. *Exp Neurol* 2015;273:301–311.
49. Hong S, Fan J, Kemmerer ES, Evans S, Li Y, Wiley JW. Reciprocal changes in vanilloid (TRPV1) and endocannabinoid (CB1) receptors contribute to visceral hyperalgesia in the water avoidance stressed rat. *Gut* 2009;58:202–210.
50. Ibeakanma C, Ochoa-Cortes F, Miranda-Morales M, McDonald T, Spreadbury I, Cenac N, Cattaruzza F, Hurlbut D, Vanner S, Bunnett N, Vergnolle N, Vanner S. Brain-gut interactions increase peripheral nociceptive signaling in mice with postinfectious irritable bowel syndrome. *Gastroenterology* 2011;141:2098–2108 e5.

51. Gustafsson JK, Greenwood-Van Meerveld B. Amygdala activation by corticosterone alters visceral and somatic pain in cycling female rats. *Am J Physiol Gastrointest Liver Physiol* 2011;300:G1080–G1085.
52. Basso L, Lapointe TK, Iftinca M, Marsters C, Hollenberg MD, Kurrasch DM, Altier C. Granulocyte-colony-stimulating factor (G-CSF) signaling in spinal microglia drives visceral sensitization following colitis. *Proc Natl Acad Sci U S A* 2017;114:11235–11240.
53. Johnson AC, Greenwood-Van Meerveld B. Knockdown of steroid receptors in the central nucleus of the amygdala induces heightened pain behaviors in the rat. *Neuropharmacology* 2015;93:116–123.
54. Jain P, Hassan AM, Koyani CN, Mayerhofer R, Reichmann F, Farzi A, Schuligoi R, Malle E, Holzer P. Behavioral and molecular processing of visceral pain in the brain of mice: impact of colitis and psychological stress. *Front Behav Neurosci* 2015;9:177.
55. Shen S, Lim G, You Z, Ding W, Huang P, Ran C, Doheny J, Caravan P, Tate S, Hu K, Kim H, McCabe M, Huang B, Xie Z, Kwon D, Chen L, Mao J. Gut microbiota is critical for the induction of chemotherapy-induced pain. *Nat Neurosci* 2017;20:1213–1216.
56. Yang C, Fang X, Zhan G, Huang N, Li S, Bi J, Jiang R, Yang L, Miao L, Zhu B, Luo A, Hashimoto K. Key role of gut microbiota in anhedonia-like phenotype in rodents with neuropathic pain. *Transl Psychiatry* 2019;9:57.
57. Aminoglycosides. *LiverTox: clinical and research information on drug-induced liver injury*. Bethesda, MD: National Institute of Diabetes and Digestive and Kidney Diseases, 2012.
58. Selimoglu E. Aminoglycoside-induced ototoxicity. *Curr Pharm Des* 2007;13:119–126.
59. Goolsby TA, Jakeman B, Gaynes RP. Clinical relevance of metronidazole and peripheral neuropathy: a systematic review of the literature. *Int J Antimicrob Agents* 2018; 51:319–325.
60. O'Mahony SM, Felice VD, Nally K, Savignac HM, Claesson MJ, Scully P, Woznicki J, Hyland NP, Shanahan F, Quigley EM, Marchesi JR, O'Toole PW, Dinan TG, Cryan JF. Disturbance of the gut microbiota in early-life selectively affects visceral pain in adulthood without impacting cognitive or anxiety-related behaviors in male rats. *Neuroscience* 2014;277:885–901.
61. Luczynski P, Tramullas M, Viola M, Shanahan F, Clarke G, O'Mahony S, Dinan TG, Cryan JF. Microbiota regulates visceral pain in the mouse. *Elife* 2017;6.
62. Johnson AC, Greenwood-Van Meerveld B, McRorie J. Effects of *Bifidobacterium infantis* 35624 on post-inflammatory visceral hypersensitivity in the rat. *Dig Dis Sci* 2011;56:3179–3186.
63. Perez-Burgos A, Wang L, McVey Neufeld KA, Mao YK, Ahmadzai M, Janssen LJ, Stanis AM, Bienenstock J, Kunze WA. The TRPV1 channel in rodents is a major target for antinociceptive effect of the probiotic *Lactobacillus reuteri* DSM 17938. *J Physiol* 2015; 593:3943–3957.
64. Tan J, McKenzie C, Potamitis M, Thorburn AN, Mackay CR, Macia L. The role of short-chain fatty acids in health and disease. *Adv Immunol* 2014;121:91–119.
65. Duvallet C, Gibbons SM, Gurry T, Irizarry RA, Alm EJ. Meta-analysis of gut microbiome studies identifies disease-specific and shared responses. *Nat Commun* 2017;8:1784.
66. Geirnaert A, Calatayud M, Grootaert C, Laukens D, Devriese S, Smagge G, De Vos M, Boon N, Van de Wiele T. Butyrate-producing bacteria supplemented in vitro to Crohn's disease patient microbiota increased butyrate production and enhanced intestinal epithelial barrier integrity. *Sci Rep* 2017;7:11450.
67. Vich Vila A, Imhann F, Collij V, Jankipersadsing SA, Gurry T, Mujagic Z, Kurilshikov A, Bonder MJ, Jiang X, Tigchelaar EF, Dekens J, Peters V, Voskuil MD, Visschedijk MC, van Dullemen HM, Keszthelyi D, Swertz MA, Franke L, Alberts R, Festen EAM, Dijkstra G, Masclee AAM, Hofker MH, Xavier RJ, Alm EJ, Fu J, Wijmenga C, Jonkers D, Zhernakova A, Weersma RK. Gut microbiota composition and functional changes in inflammatory bowel disease and irritable bowel syndrome. *Sci Transl Med* 2018;10.
68. Mearin F, Lacy BE, Chang L, Chey WD, Lembo AJ, Simren M, Spiller R. Bowel disorders. *Gastroenterology* 2016;13:501–502.
69. Rajilic-Stojanovic M, Biagi E, Heilig HG, Kajander K, Kekkonen RA, Tims S, de Vos WM. Global and deep molecular analysis of microbiota signatures in fecal samples from patients with irritable bowel syndrome. *Gastroenterology* 2011;141:1792–1801.
70. Bennet SM, Ohman L, Simren M. Gut microbiota as potential orchestrators of irritable bowel syndrome. *Gut Liver* 2015;9:318–331.
71. Pittayanon R, Lau JT, Yuan Y, Leontiadis GI, Tse F, Surette M, Moayyedi P. Gut microbiota in patients with irritable bowel syndrome: a systematic review. *Gastroenterology* 2019;157:97–108.
72. Labus JS, Osadchij V, Hsiao EY, Tap J, Derrien M, Gupta A, Tillisch K, Le Neve B, Grinsvall C, Ljungberg M, Ohman L, Tornblom H, Simren M, Mayer EA. Evidence for an association of gut microbial *Clostridia* with brain functional connectivity and gastrointestinal sensorimotor function in patients with irritable bowel syndrome, based on tripartite network analysis. *Microbiome* 2019;7:45.
73. Krogus-Kurikka L, Lyra A, Malinen E, Aarnikunnas J, Tuimala J, Paulin L, Makivuokko H, Kajander K, Palva A. Microbial community analysis reveals high level phylogenetic alterations in the overall gastrointestinal microbiota of diarrhoea-predominant irritable bowel syndrome sufferers. *BMC Gastroenterol* 2009;9:95.
74. Salonen A, de Vos WM, Palva A. Gastrointestinal microbiota in irritable bowel syndrome: present state and perspectives. *Microbiology* 2010;156:3205–3215.
75. Hollister EB, Oezguen N, Chumpitazi BP, Luna RA, Weidler EM, Rubio-Gonzales M, Dahdouli M, Cope JL, Mistretta TA, Raza S, Metcalf GA, Muzny DM, Gibbs RA, Petrosino JF, Heitkemper M, Savidge TC, Shulman RJ, Versalovic J. Leveraging human microbiome features to diagnose and stratify children with irritable bowel syndrome. *J Mol Diagn* 2019; 21:449–461.

76. Primec M, Micetic-Turk D, Langerholc T. Analysis of short-chain fatty acids in human feces: a scoping review. *Anal Biochem* 2017;526:9–21.
77. Cox SR, Lindsay JO, Fromentin S, Stagg AJ, McCarthy NE, Galleron N, Ibraim SB, Roume H, Levenez F, Pons N, Maziers N, Lomer MC, Ehrlich SD, Irving PM, Whelan K. Effects of low FODMAP diet on symptoms, fecal microbiome, and markers of inflammation in patients with quiescent inflammatory bowel disease in a randomized trial. *Gastroenterology* 2020;158:176–188 e7.
78. Aden K, Rehman A, Waschina S, Pan WH, Walker A, Lucio M, Nunez AM, Bharti R, Zimmerman J, Bethge J, Schulte B, Schulte D, Franke A, Nikolaus S, Schroeder JO, Vandeputte D, Raes J, Szymczak S, Waetzig GH, Zeuner R, Schmitt-Kopplin P, Kaleta C, Schreiber S, Rosenstiel P. Metabolic functions of gut microbes associate with efficacy of tumor necrosis factor antagonists in patients with inflammatory bowel diseases. *Gastroenterology* 2019;157:1279–1292 e11.
79. Halmos EP, Christophersen CT, Bird AR, Shepherd SJ, Gibson PR, Muir JG. Diets that differ in their FODMAP content alter the colonic luminal microenvironment. *Gut* 2015;64:93–100.
80. Sakata T. Pitfalls in short-chain fatty acid research: a methodological review. *Anim Sci J* 2019;90:3–13.
81. Gill PA, van Zelm MC, Muir JG, Gibson PR. Review article: short chain fatty acids as potential therapeutic agents in human gastrointestinal and inflammatory disorders. *Aliment Pharmacol Ther* 2018;48:15–34.
82. Xu D, Wu X, Grabauskas G, Owyang C. Butyrate-induced colonic hypersensitivity is mediated by mitogen-activated protein kinase activation in rat dorsal root ganglia. *Gut* 2013;62:1466–1474.
83. Tarrerias AL, Millecamps M, Alloui A, Beaughard C, Kemeny JL, Bourdu S, Bommelaer G, Eschaliere A, Dapoigny M, Ardid D. Short-chain fatty acid enemas fail to decrease colonic hypersensitivity and inflammation in TNBS-induced colonic inflammation in rats. *Pain* 2002;100:91–97.
84. Vanhoutvin SA, Troost FJ, Kilkens TO, Lindsey PJ, Hamer HM, Jonkers DM, Venema K, Brummer RJ. The effects of butyrate enemas on visceral perception in healthy volunteers. *Neurogastroenterol Motil* 2009;21, 952–e76.
85. Reijnders D, Goossens GH, Hermes GD, Neis EP, van der Beek CM, Most J, Holst JJ, Lenaerts K, Kootte RS, Nieuwdorp M, Groen AK, Olde Damink SW, Boekschooten MV, Smidt H, Zoetendal EG, Dejong CH, Blaak EE. Effects of gut microbiota manipulation by antibiotics on host metabolism in obese humans: a randomized double-blind placebo-controlled trial. *Cell Metab* 2016;24:63–74.
86. Song Z, Xie W, Chen S, Strong JA, Print MS, Wang JI, Shareef AF, Ulrich-Lai YM, Zhang JM. High-fat diet increases pain behaviors in rats with or without obesity. *Sci Rep* 2017;7:10350.
87. Barrot M. Tests and models of nociception and pain in rodents. *Neuroscience* 2012;211:39–50.
88. Cenac N, Andrews CN, Holzhausen M, Chapman K, Cottrell G, Andrade-Gordon P, Steinhoff M, Barbara G, Beck P, Bunnett NW, Sharkey KA, Ferraz JG, Shaffer E, Vergnolle N. Role for protease activity in visceral pain in irritable bowel syndrome. *J Clin Invest* 2007;117:636–647.
89. Martin M. Cutadapt removes adapter sequences from high-throughput sequencing reads. *EMBnet.Journal* 2011;17:10–12.
90. Callahan BJ, McMurdie PJ, Rosen MJ, Han AW, Johnson AJ, Holmes SP. DADA2: high-resolution sample inference from Illumina amplicon data. *Nat Methods* 2016;13:581–583.
91. Bihan D, Rydzak T, Wyss M, Pittman K, McCoy KD, Lewis IA. Method for absolute quantification of short chain fatty acids via reverse phase chromatography mass spectrometry. *ChemRxiv* 2019.
92. Clasquin MF, Melamud E, Rabinowitz JD. LC-MS data processing with MAVEN: a metabolomic analysis and visualization engine. *Curr Protoc Bioinformatics* 2012, Chapter 14:Unit14.11.
93. Melamud E, Vastag L, Rabinowitz JD. Metabolomic analysis and visualization engine for LC-MS data. *Anal Chem* 2010;82:9818–9826.
94. McMurdie PJ, Holmes S. phyloseq: an R package for reproducible interactive analysis and graphics of microbiome census data. *PLoS One* 2013;8:e61217.
95. Love MI, Huber W, Anders S. Moderated estimation of fold change and dispersion for RNA-seq data with DESeq2. *Genome Biol* 2014;15:550.

---

Received January 12, 2020. Revised April 1, 2020. Accepted April 3, 2020.

#### Correspondence

Address correspondence to: Yasmin Nasser, MD, PhD, 1667 Health Sciences Building, University of Calgary, 3330 Hospital Drive NW, Calgary, Alberta, Canada T2N 4N1. e-mail: ynasser@ucalgary.ca; fax: (403) 210-9657.

#### Acknowledgments

The authors acknowledge Ron Chan and Anowara Islam for their outstanding technical expertise. K.A.S. holds the Crohn's and Colitis Canada Chair in Inflammatory Bowel Disease Research at the University of Calgary.

Portions of this manuscript have been presented in abstract form at Digestive Diseases Week (DDW) and Canadian Digestive Diseases Week (CDDW).

Current address for L. Basso: Unité de Différenciation Epithéliale et Autoimmunité Rhumatoïde, UMR 1056, INSERM, University of Toulouse, Toulouse, France.

#### Author contributions

NE, KAS, CA, and YN designed the study; NE, LB, MD, FAV, NC, and DB performed the experiments; IAL and MBG provided material/experimental support; NE, AS, MD, DB, and YN analyzed and interpreted the data; NE and YN drafted the manuscript; HBJ, IAL, MBG, SAH, KAS, and CA critically revised the manuscript for important intellectual content. All authors had access to the study data and have reviewed and approved the final manuscript.

#### Conflicts of interest

The authors disclose no conflicts.

#### Funding

Supported by Crohn's and Colitis Canada (YN, HBJ, CA, SAH), the Canadian Institutes of Health Research (CA, KAS, SAH), the Department of Medicine/Division of Gastroenterology (YN, HBJ), the Cumming School of Medicine (YN), the Koopmans Memorial Research Fund (YN), and the Crohn's and Colitis Canada Chair in Inflammatory Bowel Disease Research (YN). FAV was supported by the National Council for Scientific and Technological Development, Brazil. Metabolomics data were acquired by DB at the Calgary Metabolomics Research Facility (CMRF), which is supported by the International Microbiome Centre and the Canada Foundation for Innovation. IAL is supported by an Alberta Innovates Translational Health Chair.